mineralization is discovered from the results of the current Gravity and IP field observations.

3.3.4 Laboratory Tests

Enforced wet densities of 21 rock samples collected in and around the prospect are resulted in the range between 2.02 through 3.82 g/cm^3 from density measurement in laboratory. The estimated average density of 2.67 g/cm^3 is higher than the correction density of 2.33 g/cm^3 adopted in the current gravity survey. Two celestite samples higher density than 3.5 g/cm^3 raise the average density. Hard rock samples with better property are measured in the many case of laboratory test, although many fragile rocks possibly disintegrated during shaping or immersion are lying in the field. In the current test, the four fifths of samples indicate less porosity than 10 %. Average density of rock samples decreases in order of the Cretaceous system of 2.65 g/cm^3 in, the Triassic system of 2.59 g/cm^3 and the Tertiary system 2.50 g/cm^3. The highest average density of 2.92 g/cm^3 is indicated in the rocks collected in the transition zone around the ore deposits.

The results from resistivity and chargeability measurement of 20 rock samples measured density, except for a sample disintegrated during immersion, are shown in Table 26. Resistivities ranging from 80 to 11,000 Ωm are extremely higher than the measured resistivities from the field survey of which many indicating less than 10Ωm. Rock resistivity ρr is affected by resistivity of pore water ρw and porosity ϕ, as represented following Archie's formula (Archie, 1941).

$$F=\rho r/\rho w=a\phi^{m} \qquad (16)$$

Where, F is proportional factor called the formation resistivity factor, a called tortosity factor and m called cementing factor are experimentally estimated in every geological unit. Tortosity factor indicates value around one, cementing factor is ranging between 0.8 and 2.5. As mention above, rock samples indicating lower porosity than rocks lying in fields produce the difference of results between in field survey and in laboratory test. However, extreme low resistivity resulted from the current field survey cannot be explained by only high porosity. Pore water as conductive as sea water indicating less than 1 Ωm is suggested.

Measured chargeability of rock samples is low except for two samples of sandstone indicating higher than 10mV/V. The sample 12 of limestone collecting around the old Bou Khil working is measured relative high chargeability of about 8mV/V. The samples of celestite collecting in the high chargeability zone characterized from the current field survey indicate low chargeability lower than 3.5 mV/V. Another sample collected in a waste deposit of the old Bou Khil mine indicates chargeability

considerably higher than 20 mV/V. The fact that the sample includes sulfide lead suggests that sulfide lead like galena generates high chargeability.

The cross plots on measured density, resistivity and chargeability of samples are shown in Figure 79. Resistive rock samples tend to increase density, but their correlation is weak. No valid correlation between Resistivity and chargeability is indicated.

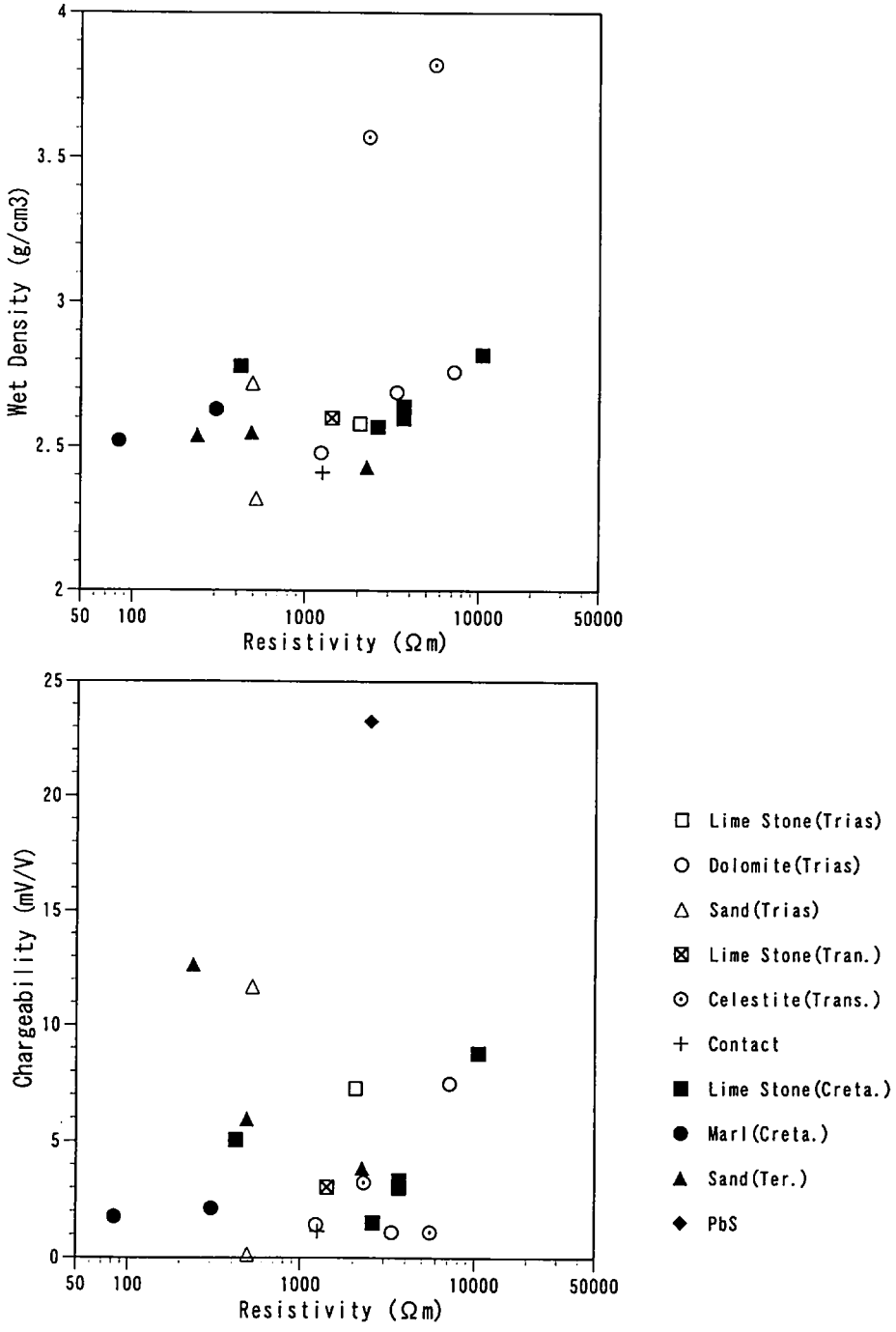

Figure 79 Cross-Plots of Results of Laboratory Measurement

Chapter 4 El Akhouat - Argoub Adama Prospect

4.1 Airphoto Analysis

The airphoto interpretation is made for the monochromatic air photographs at a scale of 1 to 25,000, obtained in the Republic of Tunisia, covering an area of 25 km^2 that includes the El Akhouat-Argoub Adama prospect. The purposes of the interpretation are to verify faults, beddings and other lineaments and to discriminate lithology in relation with the mineralization in the prospect.

The specifications of the used air photographs are shown in Table 27 and the result of interpretation is illustrated in Figure 80.

Table 27 Specifications of Air Photographs

Location	Photo No.	Number of Photos	Remarks
El Akhouat – Argoub Adama	1340-1343, 1373-1376	8 sheets	Project:74TU359/250 UAG412

A number of lineaments, which are interpreted as possible faults, are observed in association with the Triassic and Cretaceous systems. Most of them trend either in the N-S, NW-SE, NE-SW or WNW-ESE direction. Lineaments, possibly indicating beddings, are observed all of the Triassic, Cretaceous and Tertiary terrain. They trend in the NE-SW to ENE-WSW directions in the Triassic terrain, and in the N-S, NNE-SSW and NW-SE directions in the Cretaceous terrain and in the N-S direction in the Tertiary terrain.

4.2 Geological Prospecting

4.2.1 Methodology

The purpose of the geological prospecting was to investigate geology, geological structures and mineral occurrences in the prospect in order to verify dome structures with respect to Pb-Zn mineralization.

The geological prospecting was principally carried out along the measuring lines set for the geophysical prospecting, aiming at producing a geological fact map at a scale of 1 to 5,000. A topographic map at a scale of 1 to 5,000 was prepared, by enlarging a published topographic map at a scale of 1 to 50,000, for the supplemental

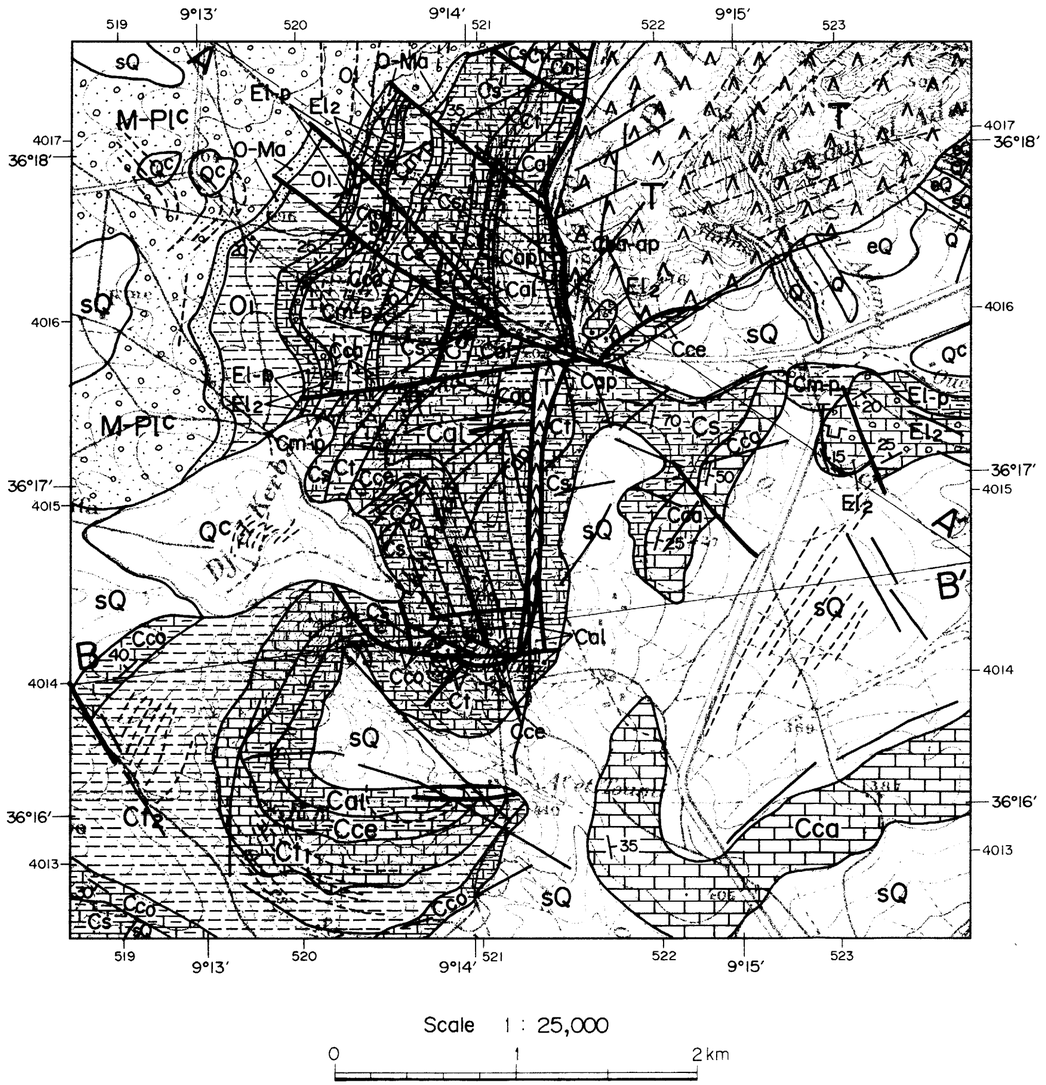

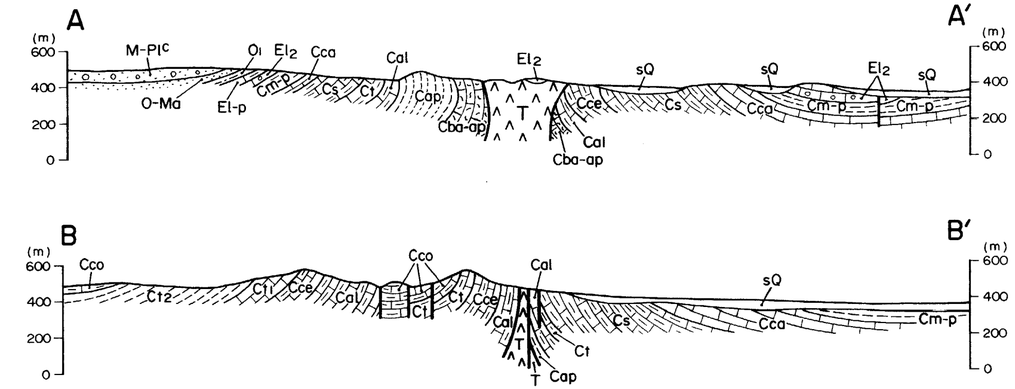

LEGEND

Quaternary	Pleistocene	eQ	rubble
	Pleistocene	sQ	soil
	Pleistocene	Qc	calcareous conglomerate
	Pleistocene	Q	siltstone, conglomerate
Tertiary	Miocene ~ Pliocene	M-Plc	sandstone, conglomerate, marl, sand, clay
	Oligocene ~ Miocene	O-Ma	sandstone
	Oligocene	Ol	marl, sandstone, limestone
	Eocene	El-p	marl, limestone
	Eocene	El2	limestone, conglomerate

Cretaceous	Maastrichtian ~Palaeocene	Cm-p	marl
	Campanian	Cca	limestone
	Santonian	Cs	marl, limestone
	Coniacian	Cco	marl, limestone
	Turonian	Ct	limestone, marl
	Turonian	Ct2	marl
	Turonian	Ct1	limestone
	Cenomanian	Cce	limestone, marl
	Albian	Cal	limestone, marl
	Aptian	Cap	marl, sandstone
	Barremian ~ Aptian	Cba-ap	marl, quartzite, limestone
Triassic		T	gypsum, clay, sandstone, dolomite, limestone

Fault

Lineament

Figure 80 Geological map and cross section of El Akhouat Prospect

prospecting along creeks and roads between the geophysical measuring lines. Rock and ore samples were collected from selected outcrops useful for identifying stratigraphy and geological structures.

The prospecting result was compiled into a geological map at a scale of 1 to 25,000, together with geological cross sections of the same scale. Collected samples were submitted for microscopic observation of thin sections and polishes, X-ray diffraction analysis and/or chemical analysis.

4.2.2 Geology

The El Akhouat-Argoub Adama prospect encompasses an area of 5x5 km, including the southern end of the Jebel Ech Cheid diapir body. The stratigraphy comprises, in its ascending order, the Triassic, Cretaceous, Tertiary and Quaternary systems. The geological plan and cross sections of the prospect are shown in Figure 80, and the schematic stratigraphic section, in Figure 81.

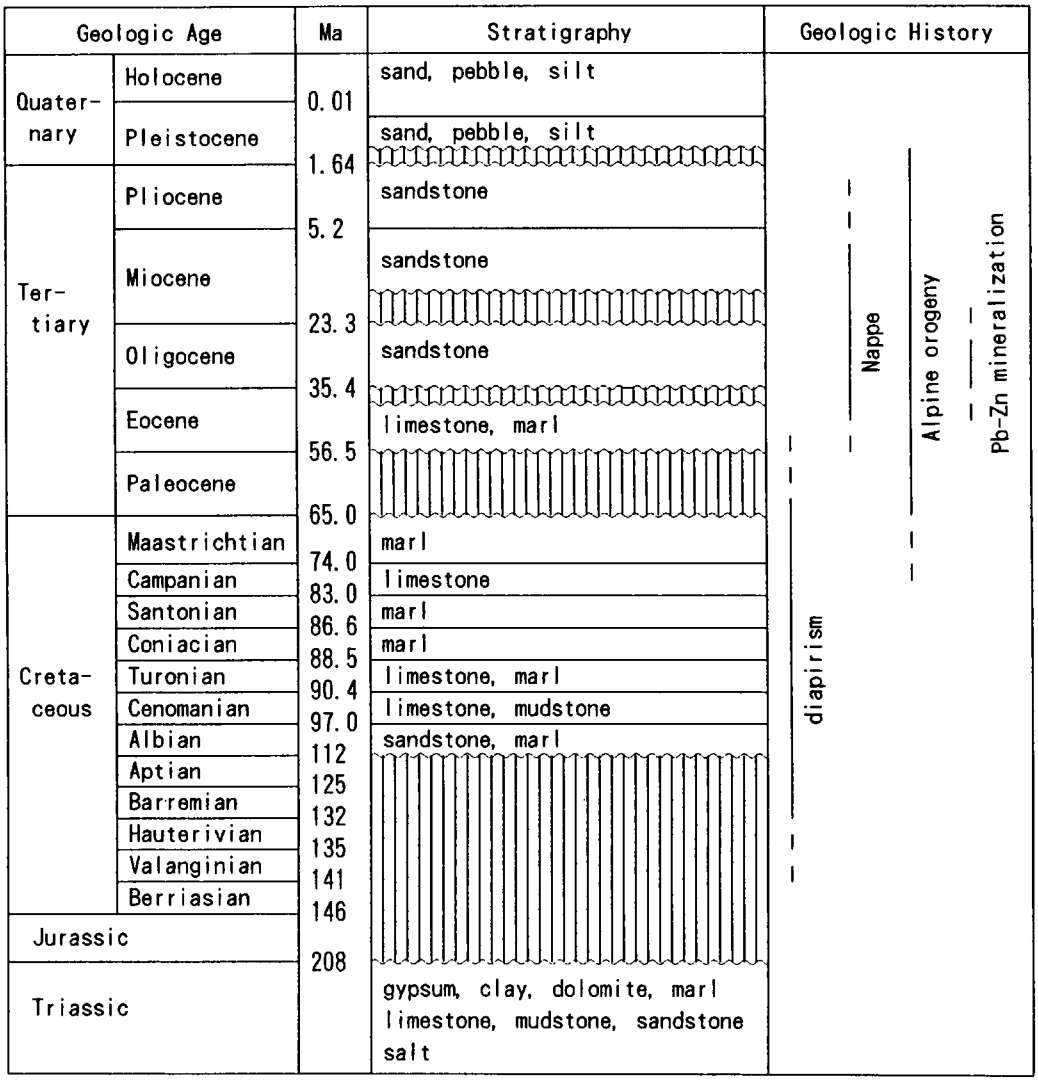

Figure 81 Schematic stratigraphic section

The Triassic system is composed of gypsum, clay, dolomite, marl, limestone, argillite and meta-sandstone. Their sedimentary structures are extremely disturbed by folding, over-folding and faulting of various scales and attitudes due to diapirism. Lithology of the Triassic system is inhomogeneous as a whole, comprising mixed blocks of various rock types and with very poor continuity of each stratum. The southwest part of Jebel Ech Cheid diapir body elongated in the NE-SW direction is bordered by faults and pinches out within the El Akhouat-Argoub Adama prospect. In the south end of these faults, Triassic system is exposed like a window along the E-W striking faults. The diapir body in the northeastern part of the prospect, forming a mushroom shape on its cross section, is in contact with the Cretaceous and Tertiary systems on its western side, and is covered by the Quaternary system on its southeastern side. The diapir is bordered with the Cretaceous system by faults in the central part of the prospect where the exposure of the diapir is terminated.

The Cretaceous system comprises, in stratigraphically ascending order, sandstone and marl of Aptian, limestone and argillite of Albian, limestone and marl of Cenomanian, limestone of Turonian, marl of Coniacian, marl of Santonian, limestone of Campanian and marl of Maastrichtian. In the western side of the Triassic diapir, all Cretaceous formations from Aptian to Maastrichtian are exposed continuously, then both Aptian and Albian formations contact with the Triassic diapir. In the eastern side of the Triassic diapir, the Cretaceous formations from Cenomanian to Maastrichtian are exposed intermittently like a window, then Cenomanian, Turonian and Santonian formations contact with the Triassic diapir. The Aptian sandstone is coarse-grained, hard and well-stratified. The Albian formation consists of black to pinkish gray limestone partly with thin bedding and dark gray to dark greenish gray argillite fragmented by weathering. The El Akhouat ore deposits exist in the Albian limestone. The Cenomanian formation comprises grayish white well-stratified limestone and marl. The Turonian limestone is characteristically black on fresh outcrops and is called 'Bahloul' in Tunisian. The Coniacian and Santonian formations comprise grayish white and well-stratified marl. The Campanian limestone is grayish white and massive or weakly stratified. The Maastrichtian marl is grayish white and weakly stratified.

The Tertiary system comprises, in stratigraphically ascending order, Eocene limestone and marl, and Oligocene, Miocene and Pliocene sandstones. These Tertiary rocks distribute only in the northern part of the prospect surrounding the Cretaceous and Triassic systems. The Eocene limestone contains abundant Nummulites fossils. The terrestrial sandstones of Oligocene through Pliocene are porous, weakly consolidated and fine to medium grained, consisting mostly of rounded quartz grains. The Quaternary system comprises alluvial deposits, such as calcareous conglomerate,

gravel, sand and mud, and alluvial soils. The conglomerate secondarily consolidated by calcic components distributes locally in the surface of the Triassic diapir. The similar calcareous conglomerate changed from talus deposit distributes on the slope of Cretaceous formations. The foot of Jebel Ech Cheid mountain is composed of alluvial soils and utilized for cultivation.

4.2.3 Geological Structure

The Triassic diapir system takes a wedge form trending in the NE-SW to N-S direction and sharpened to the south within the prospect, and is not exposed in the south part of the prospect. The Triassic diapir system in the northern prospect, forming a mushroom shape on cross section, covers the Cretaceous system and is covered by the Quaternary system. The Triassic diapir system in the central prospect, forming a steeple shape on cross section, contacts with the Cretaceous system bordered by the N-S striking faults and pinches out in the north of the El Akhouat old mine. At the western side from the pit of the El Akhouat old mine, the Triassic system is exposed like a window bordered by the E-W striking faults and passes under the surface. At the western side of the Triassic system in the northern prospect, the Cretaceous system is intruded into by the Triassic system and has a general strike of the NNE-SSW to N-S direction and a monoclinal structure with dips of 30 to 90 degrees to west whose angle increases toward the Triassic diapir. The Tertiary system has a general strike of the NNE-SSW to NE-SW direction and a monoclinal structure continuing from the Cretaceous with dips of low angle to west. At the eastern side of the Triassic system in the northern prospect, the Cretaceous system is exposed in windows of Quaternary cover and has a general strike of the NNE-SSW to N-S direction and dips of 30 to 70 degrees to east. At the southwestern prospect, the Cretaceous system somewhat complicatedly faulted has a synclinal and anticlinal structure and dips of 30 to 70 degrees. At the east end prospect, the Tertiary system is exposed in a limited area with a small scale of synclinal structure and has a general strike of the ENE-WSW direction and dips of 10 to 20 degrees to north.

The largest geological structure within the prospect is the N-S striking fault controlling the distribution of the Triassic system. Otherwise the lateral faults running in the WNW-ESE to E-W directions are also well developed. These faults are supposed to have been created as follows. The Triassic diapir rose to become a dome while the Cretaceous formations were deposited. In the late Cretaceous a large normal fault running in the N-S direction were created and the east side of the fault relatively subsided. Under the compressive stress field on Tertiary the existed N-S striking fault had a sense of reverse-slip faulting and the right-lateral faults striking WNW-ESE to

E-W were created at the same time. The south end of the Jebel Ech Cheid diapir intruded along these faults. Although the Triassic, Cretaceous and Tertiary systems are faulted by the E-W striking lateral faults, the Cretaceous and Tertiary systems distribute continuously while transferred by faults.

The Triassic diapir in the El Akhouat-Argoub Adama prospect corresponds to the southwest end of the Jebel Ech Cheid diapir body. The diapir in the north prospect has the same general structure of the Jebel Ech Cheid diapir, but it in the south prospect has the different structure. The typical sectional models of geologic structure for the diapir existing in the Dome Zone (Perthuisot, et. al., 1999) are shown in Figure 82. The model A-B1 in the figure corresponds to the central part of the Jebel Ech Cheid diapir body and is similar to the diapir in the north prospect. The model B2 is similar to the Fedj el Adoum diapir body and also partly similar to the diapir in the south prospect.

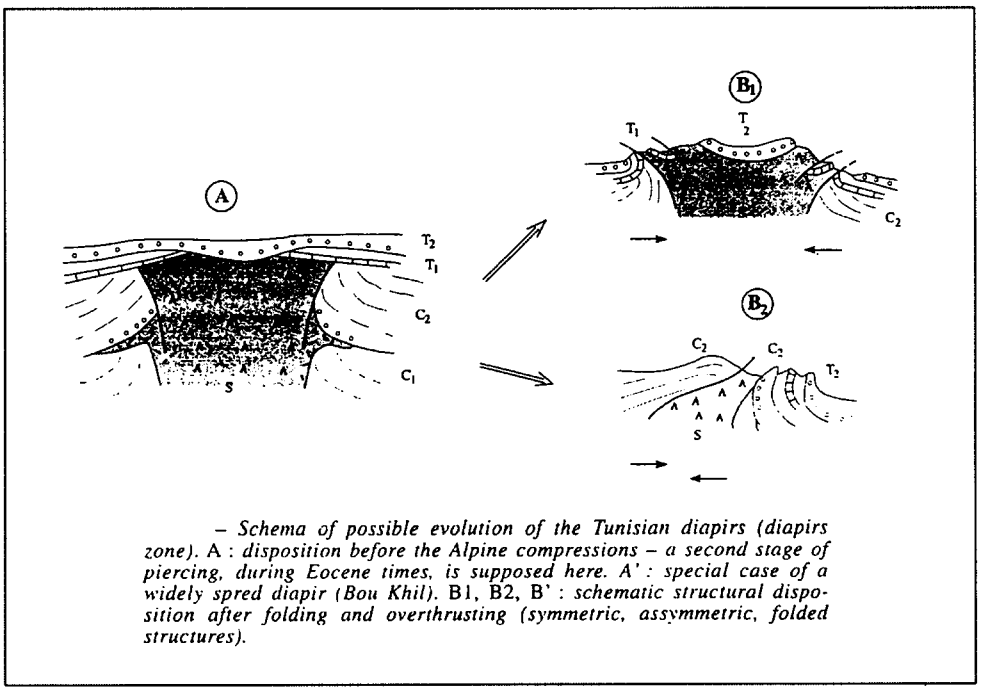

– Schema of possible evolution of the Tunisian diapirs (diapirs zone). A : *disposition before the Alpine compressions – a second stage of piercing, during Eocene times, is supposed here. A' : special case of a widely spred diapir (Bou Khil).* B1, B2, B' : *schematic structural disposition after folding and overthrusting (symmetric, assymmetric, folded structures).*

Figure 82 Sectional model of the Jebel Ech Cheid diapir (Perthuisot, et. al., 1999)

The geology and structure around the El Akhouat old mine has been vigorously investigated by National Office of Mines, the Republic of Tunisia (Mansouri, Hammami, Sellami and others) and various reports are published by them. According to these reports, the history of formation of the diapir structure can be summarized as

follows;

- The diapirism initiated in the early Cretaceous and continued to the late Tertiary.
- The diapir emerged out to the shallow sea bottom through the overlying Cretaceous system in the middle Cretaceous and took a mushroom shape. The diapir was continuously covered by the late Cretaceous system.
- In the end of Cretaceous to the beginning of Tertiary the diapir emerged out again to the shallow sea bottom through the overlying Cretaceous system.
- The top of the diapir was covered by the neritic Eocene and the continental Oligocene systems in the early Tertiary (model A in the figure 82).
- The diapirism was revitalized in Oligocene at the climax of the Alpine orogeny. The Triassic diapir exposed to the surface under the compressive stress field trending NW-SE direction and the present diapir body was formed (model B1 in the figure 82).
- A series of these movements forms the Cretaceous and Tertiary formations near the Triassic diapir into the reverse or vertical beds.

4.2.4 Mineralization

Two Pb-Zn deposits, El Akhouat and Argoub Adama, exist in the El Akhouat-Argoub Adama prospect. Both deposits are hosted in the Cretaceous limestone contacting with the Triassic diapir.

The El Akhouat deposit is located in the west side of N-S striking faults running from the south end of the Jebel Ech Cheid diapir body. The deposit is hosted in the Cretaceous Albian limestone in contact with the Triassic system of which distribution is long and narrow along the N-S striking faults. The E-W striking fault, controlling the distribution of the Triassic system, exists at the south end of the Triassic system. No ore deposit is discovered in the southern side of this E-W striking fault. The occurrence of the deposit is veins to veinlets along the limestone bedding and cracks. Ore minerals are galena, sphalerite and pyrite, and gangue minerals are calcite and dolomite. Principal veins are located within an area of 400m x 200m and the width of veins is several centimeters to several meters. The E-W striking veins are dominant and the NW-SE striking veins are also developed. The principal veins are supposed to be controlled by the large geologic structure; faults and fractures caused by the diapirism and the Alpine orogeny, and thin veins are controlled by the sedimentary structure and the small structure; bedding, cracks and small faults.

The geologic structure changes sharply at the large pit of El Akhouat old mine. The large fault running in the E-W direction exists in the pit. The Triassic system

distributes along this fault, forming a lenticular shape elongated in the E-W direction. The Triassic system distributes along the N-S striking fault in the northern side of the pit as mentioned above, but does not distribute in the south side of the E-W striking fault. Therefore, the Triassic system forms a reverse shape of 'L' by these two faults which control the Triassic distribution. The outcrop of the Triassic system running to the west from the pit pinches out by faults. The Triassic system, however, is confirmed to exist under the surface in the gallery located in the west extension from the Triassic system. The Pb-Zn ore indication is recognized around the west end of this Triassic system. Some ore samples were collected for chemical analysis in the pit. The result of chemical analysis is shown in the table 28.

Table 28 Analytical Result of Ore Samples (El Akhouat)

Sample No.	Cu (ppm)	Pb (%)	Zn (%)	Fe (%)	Mn (ppm)	Cd (ppm)	Mg (%)	Ca (%)	Sr (ppm)	Ba (ppm)	Ag (ppm)
EAK04C	29.3	0.24	17.00	2.68	1440	374.4	4.70	16.79	1525	110	1.68
EAK08C	41.5	0.15	3.20	6.41	1241	47.8	0.12	29.19	500	81	<0.3
EAK09C	1.9	0.26	12.70	7.96	3831	407.4	0.07	22.00	2269	1514	<0.3
EAK10C	4.8	10.40	2.25	0.74	607	163.6	0.20	27.19	4766	270	3.86
EAK11C	9.1	33.00	2.70	0.70	1783	151.9	0.16	18.24	305	43	90.07

The Argoub Adama deposit is located in the southeast side of the south end of the Jebel Ech Cheid diapir body. The deposit is hosted in the Cretaceous Cenomanian limestone and marl, and is composed of thin veins of galena, sphalerite, pyrite and calcite filling the cracks and along the bedding. The scale of the deposit confirmed is small; 30 to 40m in the strike extension and 10m in the dip extension. Some waste samples were collected for chemical analysis in the dump. The result of chemical analysis is shown in the table 29.

Table 29 Analytical Result of Ore Samples (Argoub Adama)

Sample No.	Cu (ppm)	Pb (%)	Zn (%)	Fe (%)	Mn (ppm)	Cd (ppm)	Mg (%)	Ca (%)	Sr (ppm)	Ba (ppm)	Ag (ppm)
EAK12C	10.9	4.84	0.52	0.88	1633	31.8	0.14	28.58	4144	754	11.9
EAK13C	15.5	2.74	0.72	1.60	1985	29.5	0.45	29.78	2569	3814	54.4
EAK14C	5.5	2.90	0.59	1.79	1457	19.9	2.90	27.99	5236	306	16.2
EAK15C	32.8	9.20	8.30	1.69	1155	829.5	2.10	22.99	1611	815	50.1

A general model of mineralization is mentioned above in the clause 3.2.4. The occurrence model of the El Akhouat deposit is estimated as follows. While the Cretaceous system were deposited and the Triassic diapir rose, the fluids including Pb-Zn in the basin of the Cretaceous system moved toward the diapir and went up along the edge of the diapir. The N-S striking normal fault was created in the late Cretaceous and the WNW-ESE to E-W striking lateral faults were developed under the compressive stress field in the late Tertiary. Then, the particular limestone, which had many fractures and were in contact with the Triassic system, selectively hosted ore deposits. The Albian limestone hosting the El Akhouat deposit is black in color and rich in organic matters or thinly well-stratified. These features are supposed to have been effective when ore deposits were formed.

4.3 Geophysical Prospecting

In the El Akhouat prospect, geophysical surveys using a gravity, IP and magnetic methods are carried out along 14 measuring lines with a total line length of 16.35 km covering an area of 3 km^2 as shown in Figure 25. The methodology and the results of the geophysical surveys are described below.

4.3.1 Methodology

(1) Layout of Measuring Lines

The 14 measuring lines, the line numbers from L0 through L13, are laid out by open traverse surveying using an electro-optical distance meter and a transit compass. Each measuring station identifies itself by the number of relevant line and one tenth of the distance from the initial station of the line. The specifications and locations of each measuring line are shown in Table 30 and Figure 83 respectively.

The baseline L0 with a total length of 3,000 m is set connecting between the old tunnel site of Argoub Adama and the old mine site of El Akhouat. The baseline which runs in the N 28° E direction is along the boundary between the Triassic and Cretaceous systems except the central parts of the line. Measuring stations of the baseline are set principally at an interval of 50 m initiated at the southwestern site.

The 14 measuring lines, which are principally 1,000 m long each and crosscut the baseline principally at its middle, are laid out perpendicularly to the baseline at an interval of 250 m with the initial stations at their northwestern ends. The lines, L7 and L8, which are extended for 200m northwestwards and crosscut the baseline at 700m from the initial station.

The coordinates of these measuring lines are determined by surveying to the

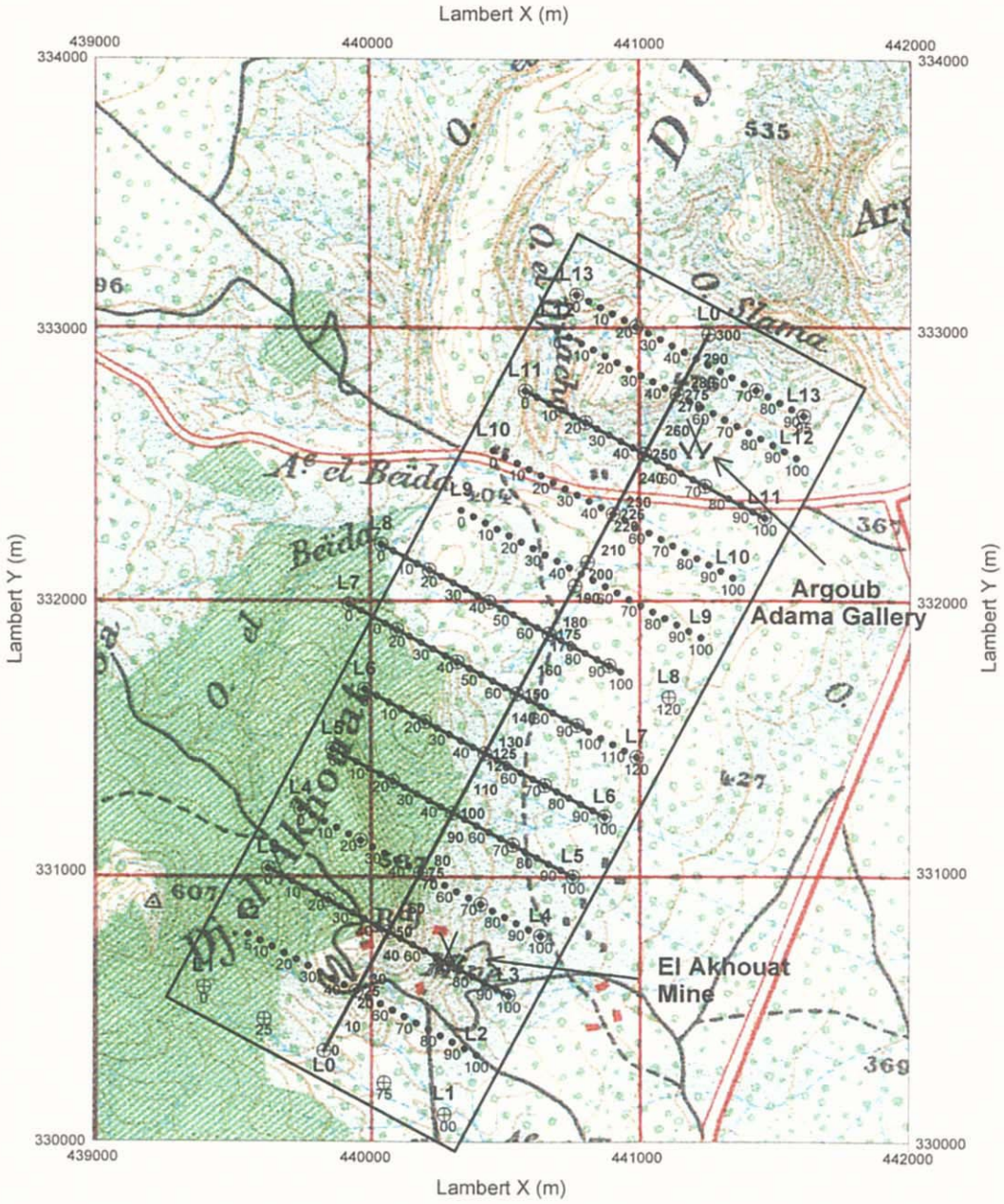

Legend

⊕ : Gravimetric Survey Station

—— : IP survey Line

• : Magnetic Survey Station

□ : Survey Area

XX : Closed Mine

Figure 83

Layout of Geophysical Survey Line in El Akhouat-Argoub Adama area

Scale 1 : 25,000

March, 2000

base station, which has been located in the vicinity of the station L0-150 by ONM. Since the coordinate system used for the surveying is the same Lambert Coordinate System as Bou Khil prospect, all coordinates are transformed to the UTM and the geophysical maps are drawn up in accordance with the Lambert Coordinate System.

The elevation of each measuring station except the L2, L9, L10 and L12, which are prepared only for the magnetic method, is determined by leveling. The leveling is carried out based on the elevation of the ONM base station located in the vicinity of the station L0-150.

Table 30 Specification of geophysical survey lines in El Akhouat area

Line	Stations	Length (km)	Angle	Crossing to L0	x(UTM)	y (UTM)	Line in Site	Applied Survey
L0	61 (0~300)	3	N28°E		520688.32	4013813.53	L0	Gravity IP
					522073.92	4016474.24		
L1	5 (0~100)	1	N62°W	L0-0	520244.86	4014044.46	L1	Gravity
					521131.78	4013582.60		
L2	20 (5~100)	1	N62°W	L0-25	520434.08	4014218.38	L25	Mag.
					521276.66	4013779.62		
L3	21 (0~100)	1	N62°W	L0-50	520475.79	4014487.92	L2	Gravity IP, Mag.
					521362.71	4014026.06		
L4	21 (0~100)	1	N62°W	L0-75	521344.68	4014404.58	L75	Gravity Mag.
					520901.22	4014404.58		
L5	21 (0~100)	1	N62°W	L0-100	520697.48	4015931.28	L3	Gravity IP, Mag.
					521584.40	4015469.42		
L6	21 (0~100)	1	N62°W	L0-125	520822.19	4015153.09	L8	Gravity IP, Mag.
					521709.11	4014691.23		
L7	25 (0~120)	1.2	N62°W	L0-150	520760.28	4015467.20	L4	Gravity IP, Mag.
					521824.58	4014912.96		
L8	25 (0~120)	1.2	N62°W	L0-175	520875.75	4015688.92	L9	Gravity IP, Mag.
					521940.05	4015134.68		
L9	21 (0~100)	1	N62°W	L0-200	521403.87	4015620.59	L200	Mag.
					522290.79	4015158.73		
L10	21 (0~100)	1	N62°W	L0-225	521548.75	4015817.60	L225	Mag.
					522435.67	4015355.74		
L11	21 (0~100)	1	N62°W	L0-250	521399.53	4016261.72	L5	Gravity IP, Mag.
					522286.45	4015799.87		
L12	21 (0~100)	1	N62°W	L0-275	521925.43	4016329.84	L275	Mag.
					522812.35	4015867.99		
L13	21 (0~100)	1	N62°W	L0-290	521584.27	4016616.48	L6	Gravity Mag.
					522426.84	4016177.72		

(2) Gravity Survey

The gravity measurements are done principally at an interval of 250 m along the 10 measuring lines, L0, L1, L3, L4, L5, L6, L7, L8 and L11. The measuring stations are totally 52 points. The El Akhouat prospect is located in the extent of the same Gafour gravity quadrangle as the Bou Khil prospect.

Relative gravity to that at the base station 12 for the Project CG-02 is measured using a gravimeter, Model D manufactured by La Coste & Romberg Co., Ltd.

Gravity is measured once or more every day at the gravity base station for each closing gravity traverse. The maximum error for a base tie measurement is 0.1 mgal throughout the current survey. The density, which is used for the Bouguer and topographic corrections, is determined by the same procedure as the Bou Khil prospect and the correction density of 2.33 g/cm^3, which was used in the Project CG-02, is adopted in the current gravity survey for the purpose of comparison. The gravity contour map indicating a horizontal distribution of Bouguer gravity anomaly is shown in Figure 86.

The gravity anomaly of the survey area is interpreted to be composed of three components based on the power spectrum (figure below) with their average depths at 927m, 188m and 51 m. Since the current gravity survey is concerned with prospecting ore deposits shallower than a few kilometers, it is tried to extract a shorter wavelength, that is, the shallow component from the Bouguer anomaly map. The filter processing of first vertical derivative, which is a kind of low-cut filter, and the trend surface analysis are adopted for extracting shorter wavelength component.

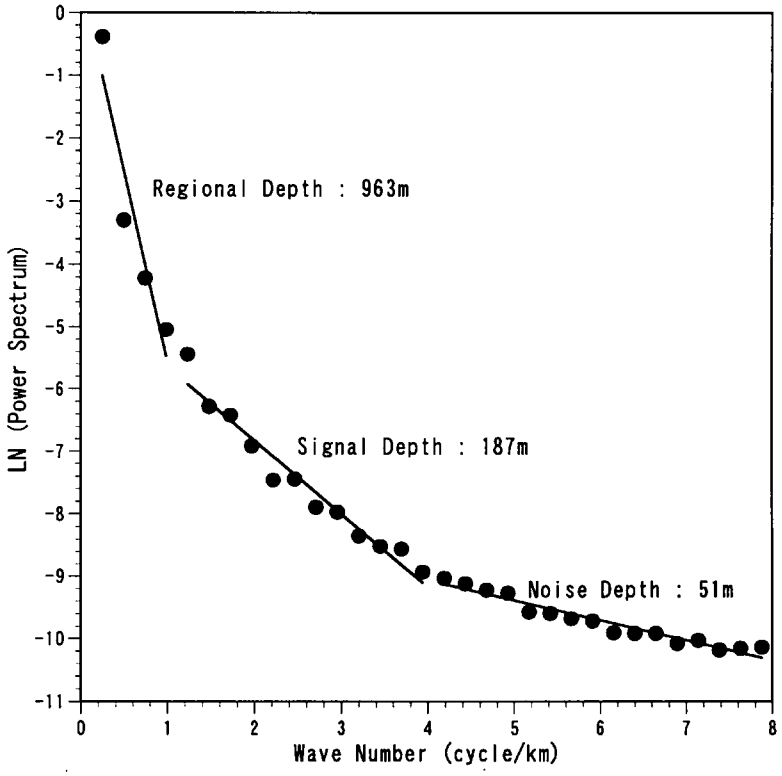

Figure 84 Power Spectrum Diagram in El Akhouat area

The gravity anomaly distribution of the CG-02 Project shown in Figure 39, in which the number of measuring stations per unit area is one quarter of the current survey or less, is utilized as the trend surface for estimation of residuals. The residual gravity anomaly map is shown in Figure 87. The first vertical derivative map is shown

in Figure 88.

A profile analysis to match the gravity residuals with the subsurface density structures along the 8 measuring lines, L0, L3, L4, L5, L6, L7, L8 and L11, is done using the GM-SYS for magnetic and gravity profile analysis. The model profiles of subsurface density structures, as the results of profile analysis, are shown in Figures 89 through 96. In the 7 lines except L0, the profile analysis is carried out jointly for the gravity and magnetic data.

(3) IP Survey

The IP survey is carried out for the 7 measuring lines, L0, L3, L5, L6, L7, L8 and L11. The line L0 is surveyed for the entire 3 km, while the measurement is made only for the northwestern end 1 km. The specifications of the IP survey and IP equipment are the same as those adopted in the Bou Khil prospect.

Pseudo-cross sections of apparent resistivity and chargeability for each measuring line are shown in Figures 98 through 104. The apparent resistivity and chargeability plan maps for the electrode separation indexes n =1,2,3 and 4 are shown in Figures 105 through 108 and Figures 109 through 112.

In the 7 measuring lines, field data are analyzed by the same technique as that in the Bou Khil prospect. Interpreted apparent resistivity and chargeability are plotted in the cross sections of measuring lines and are shown in Figures 113 through 119. Contour plans of an interpreted apparent resistivity and chargeability for elevations at 200, 300 and 400 m are shown in Figures 120 through 125 respectively.

(4) Magnetic survey

Ground magnetic measurements are carried out for the 11 lines, L2 through L11, using the proton-resonance Magnetometer MP-2 manufactured by Scintrex, Canada. Total earth magnetic intensity is measured at each measuring station and the observed value in the field is determined taking an average between three reasonable readings selected from five readings in principle. The diurnal variations of geomagnetic filed are observed during the survey every 5 minutes at the fixed station set up in the vicinity of the measuring station L8-50 using the another MP-2 magnetometer. The observed geomagnetic variations are shown in Figure 85. The diurnal corrections are made for all data obtained in the measuring lines using the readings of the fixed station corresponding to the time when the readings are obtained at each station.

Total intensities of the International Geomagnetic Reference Field are calculated for the measuring time at each station using the soft-wear NGRF by Northwest Geophysical Associates, USA. The IGRF residuals, which are applied for the

following data analysis, are obtained from the differences between the data corrected the diurnal variation and the IGRF.

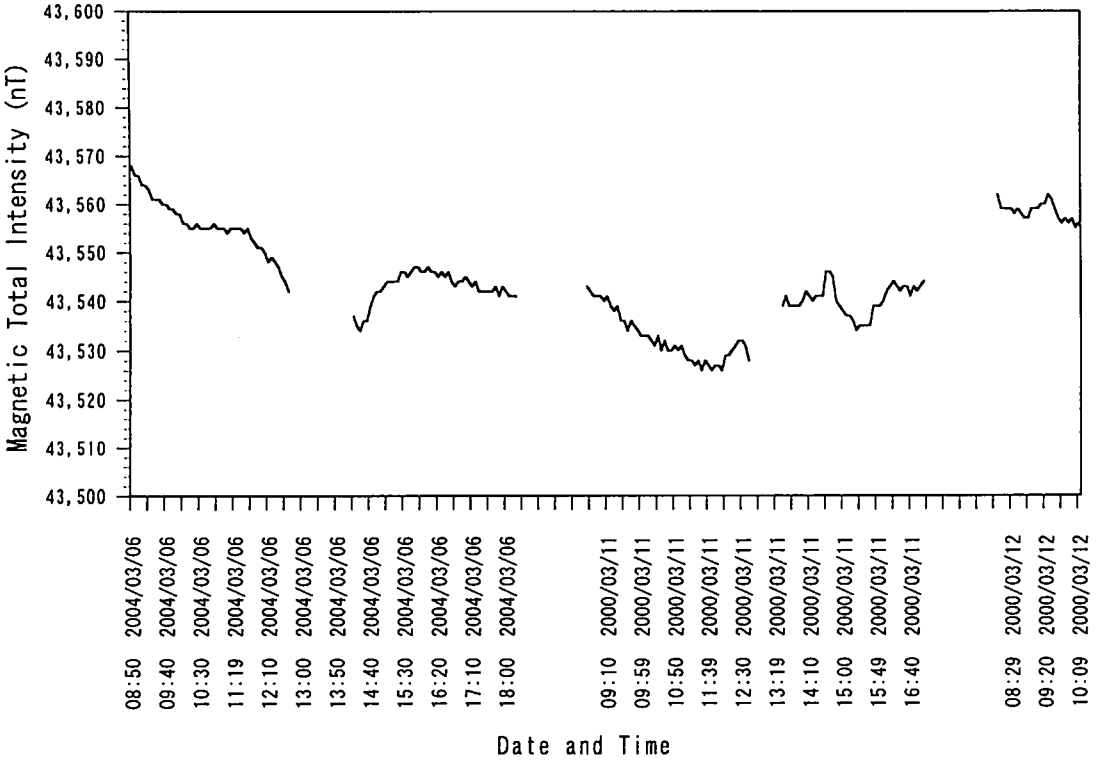

Figure 85 Time Series of Geomagnetic Variation

The contoured plan of total magnetic intensities is shown in Figure 127. The magnetic profiles along the measuring lines are shown in Figure 128. The same analytic techniques for extracting the shorter wavelength component as those used in the gravity data analysis is applied in the magnetic data processing and the first vertical derivative map drawn from the magnetic anomaly distribution is shown in Figure 129.

In the 7 measuring lines, L3, L4, L5, L6, L7, L8 and L11, the profile analysis are carried out jointly for the gravity and magnetic data using the soft-wear GMSYS as described previously in the gravity survey paragraph. The results of profile analysis are shown together with the gravity results in addition to the magnetic profiles in Figures 90 through 96.

(5) Laboratory Test

Density, resistivity and chargeability are measured in laboratory for 20 samples collected from outcrops within and around the survey area and shaped into

cylinders with a diameter of 3.5 cm and a length of 6.5 cm. Magnetic susceptibility is measured for 31 samples collected separately from above samples and shaped into cylinders with a diameter of 3.5 cm and a length between 4.0 and 6.5 cm. The corrections for diameter and porosity are made for an average susceptibility taking from three readings by the Bison susceptibility meter 3101.

The natural remnant magnetization and susceptibility for the 11 samples fixed the magnetic north and horizontal plane at the sampling site are measured using full auto spinner magnetometer, JR-5A, and the spinner kappa bridge susceptibility, KLY-3S, manufactured by AGICO, Czech Republic.

4.3.2 Gravity Survey

Characteristics of gravity anomaly distribution are described below.

(1) Regional Gravity Distributions (Figure 38 and Figure 39)

The extensive high gravity exceeding 0 mgal, which lies in the southeastern side of the survey area, extends to the WSW-ENE direction and is jutting out towards the Bou Khil prospect located in the northwestern side. In addition, the long and narrow high gravity zone extends from the high gravity jut to the northeastwards. The survey area is located in the southwestern margin of the narrow gravity high.

Taking view of the regional gravity, the Argoub Adama and the old mine site of El Akhouat are situated on a zone of steep gravity gradient where relatively high gravity exceeding -5mgals, extending to the NW-SE direction, changes to the gravity low in the northeastern parts.

(2) Gravity Distributions of the Survey Area (Figure 86)

The gravity high extending to the southwestern parts of the survey area indicates -1.25 mgals, which is a maximum value in the vicinity of measuring station L0-50 situated in the southwestern parts of the survey area. The gravity high extends to the north from near the maximum point in the western parts of the survey area. In the eastern side of this gravity high, the gravity changes rapidly from high to low and forms the zone of steep gravity gradient running from north to south.

Directions of both the gravity high and zone of steep gravity gradient agree with the strike of geological structures. In the northern parts of the old tunnel site of Argoub-Adama, the contour width of zone of steep gravity gradient trends to become wider in the distribution extent of the Triassic. In the western side of this gravity high, the gravity decreases gradually towards the gravity low extending to the northwestern parts of the survey area.

(3) Residual Gravity Anomaly (Figure 87)

The gravity residual distribution is characterized by high gravity residual, which has the N-S direction and the higher value than 1mgal, extending over the southern and western parts of the survey area. High gravity residual, which indicates the highest value in the vicinity of the station L0-100 situated at the central parts of the survey area, is correlated with the distribution zone of the Cretaceous limestone. In and around the stations L11-25 in the northern parts, L6-45 and L0-125 in the central parts and L0-125, where the Triassic is distributed, a constricted part of local gravity residual low is observed inside of high gravity residual.

The zones of steep gravity gradient, which are situated on both eastern and western sides of high gravity residual, indicate regionally the N-S direction. The zones of steep gravity gradient also indicate partially the roughness being in line of the E-W direction in the vicinity of the eastern station L6-100, the northern station L0-250 and so on. In addition, those indicate the NE-SW direction in the southeastern parts of the steep gravity gradient zone. The zone of the steep gravity gradient with the NW-SE direction lies with small scale and its direction is correlated with the direction of fault in and around the southern side of high gravity residual.

The old mine site of the El Akhouat is situated at the extreme point of high gravity residual, where the high gravity residual juts out northwards. The old tunnel site of the Argoub-Adama is situated in and around high gravity residual jut towards east.

(4) First Vertical Derivative (Figure 88)

A contour line of 0 mgal/km, which extends to the NNE-SSW direction from near the station L12-95 to near the station L4-100 in the eastern parts of the project, is considered to be correlated with the boundary between the Triassic and Cretaceous systems. The high anomalies with small scale lie in line with the N-S direction in the western side of the 0 mgal/km contour line and with the NW-SE direction in the northeastern parts of the survey area. These high anomalies are correlated with the distributions of the Cretaceous limestone. Relatively low anomalies, correlated with the distribution of the Triassic, lie in the zone between above two lines of the high anomaly. The boundary between the Triassic and Cretaceous systems is assumed based on an arrangement of high and low anomalies in the first vertical derivative map.

The fractures with small scale are assumed to lie in and around the boundary between two high anomalies divided by a constricted low anomaly.

The old mine site of the El Akhouat is situated near by the eastern side of high anomaly zone, where the fractures with small scale are possible to lie in the vicinity of

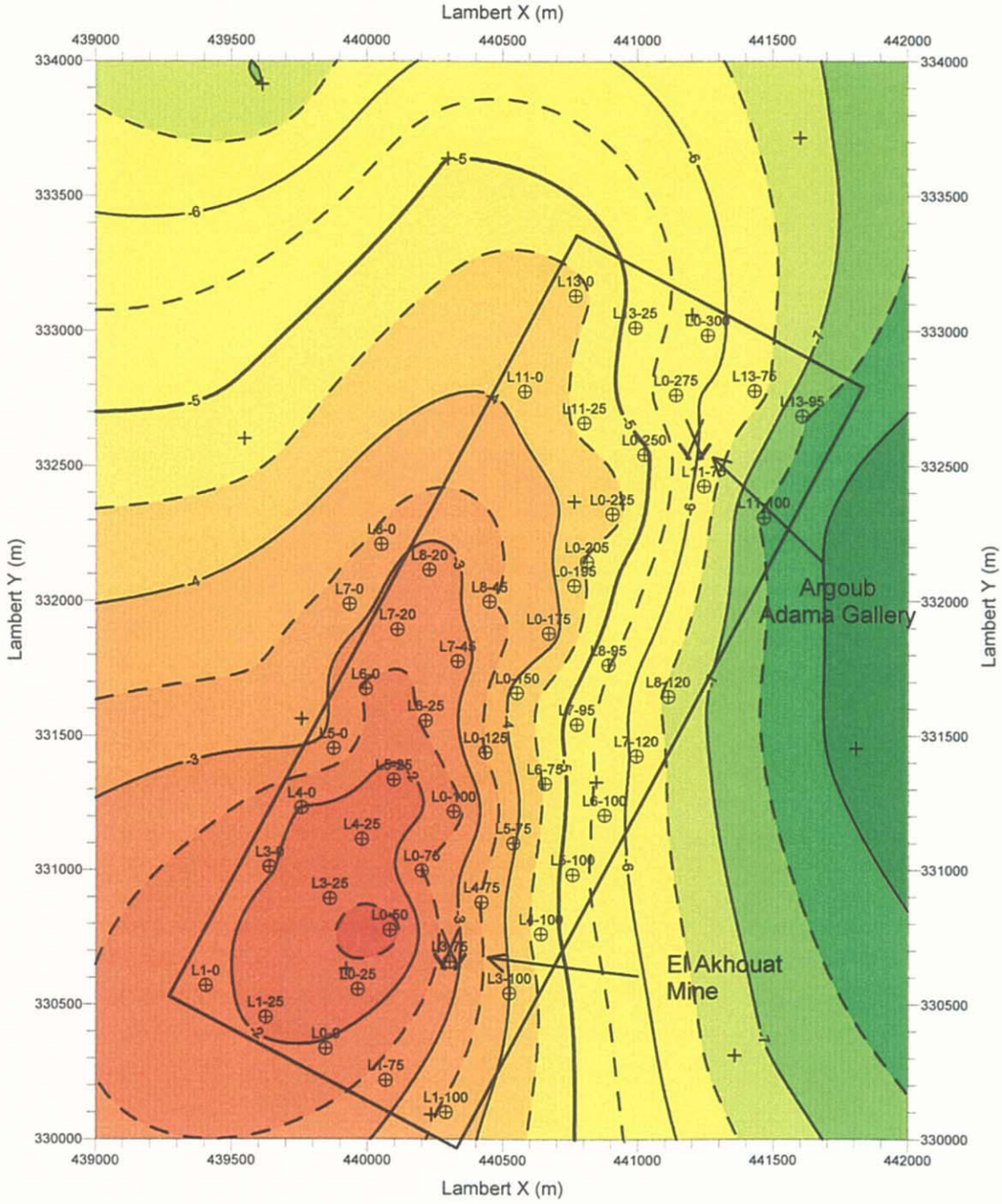

Legend

⊕ : Gravity Station

\+ : Existed Gravity Station

□ : Survey Area

XX : Closed Mine

Figure 86

Bouguer Anomaly Map in El Akhouat - Argoub Adama area (Density : 2.33 g/cm^3)

Scale 1 : 25,000

March, 2000

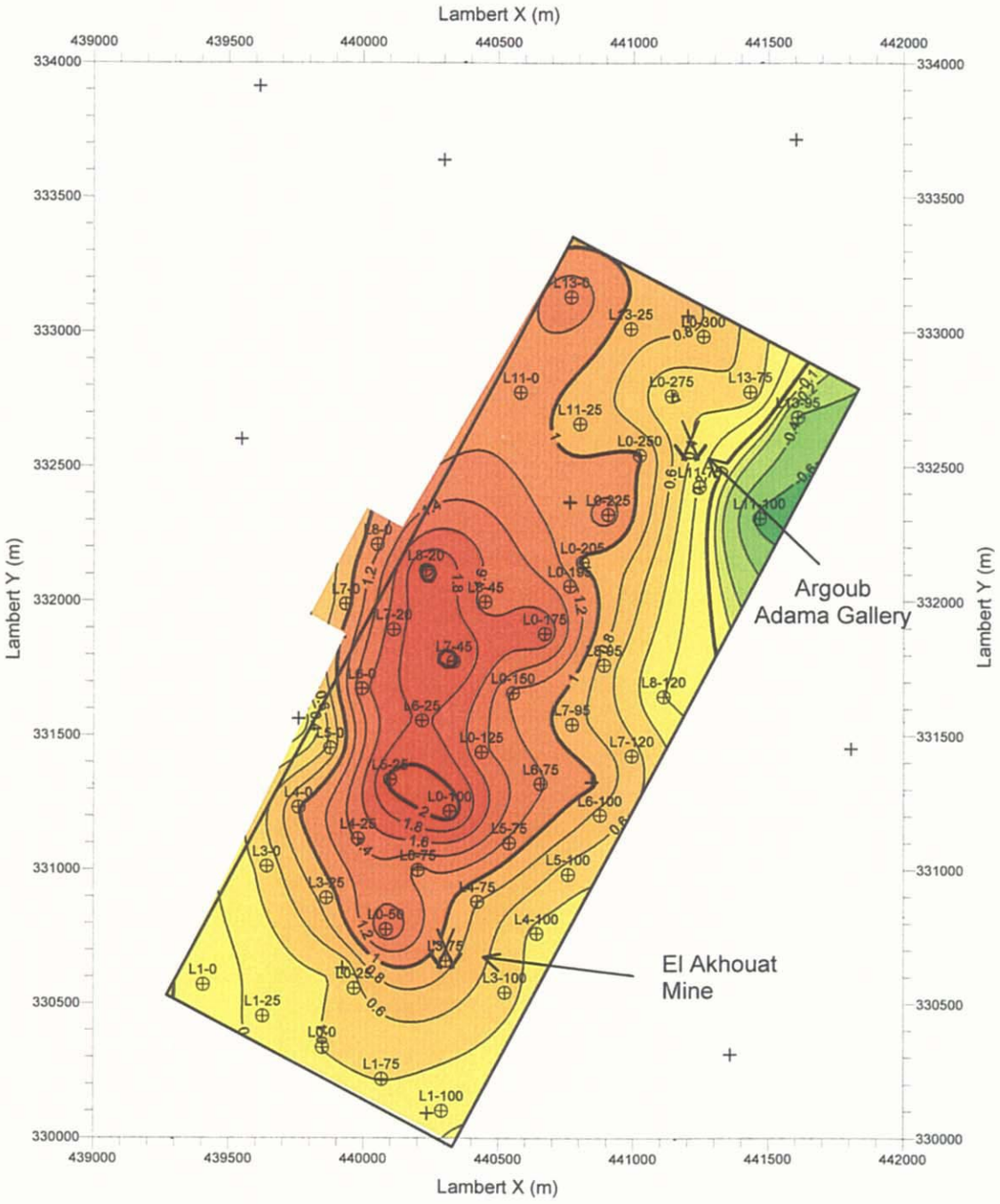

Residual Gravity
(mgal)

-2 -1.8 -1.6 -1.4 -1.2 -1 -0.8 -0.6 -0.4 -0.2 -0.1 0 0.2 0.4 0.6 0.8 1 1.2 1.4 1.6 1.8 2

Legend

⊕ : Gravity Station

\+ : Existed Gravity Station

□ : Survey Area

XX : Closed

Figure 87

Residual Gravity Map in El Akhouat - Argoub Adama area

Scale 1 : 25,000

March, 2000

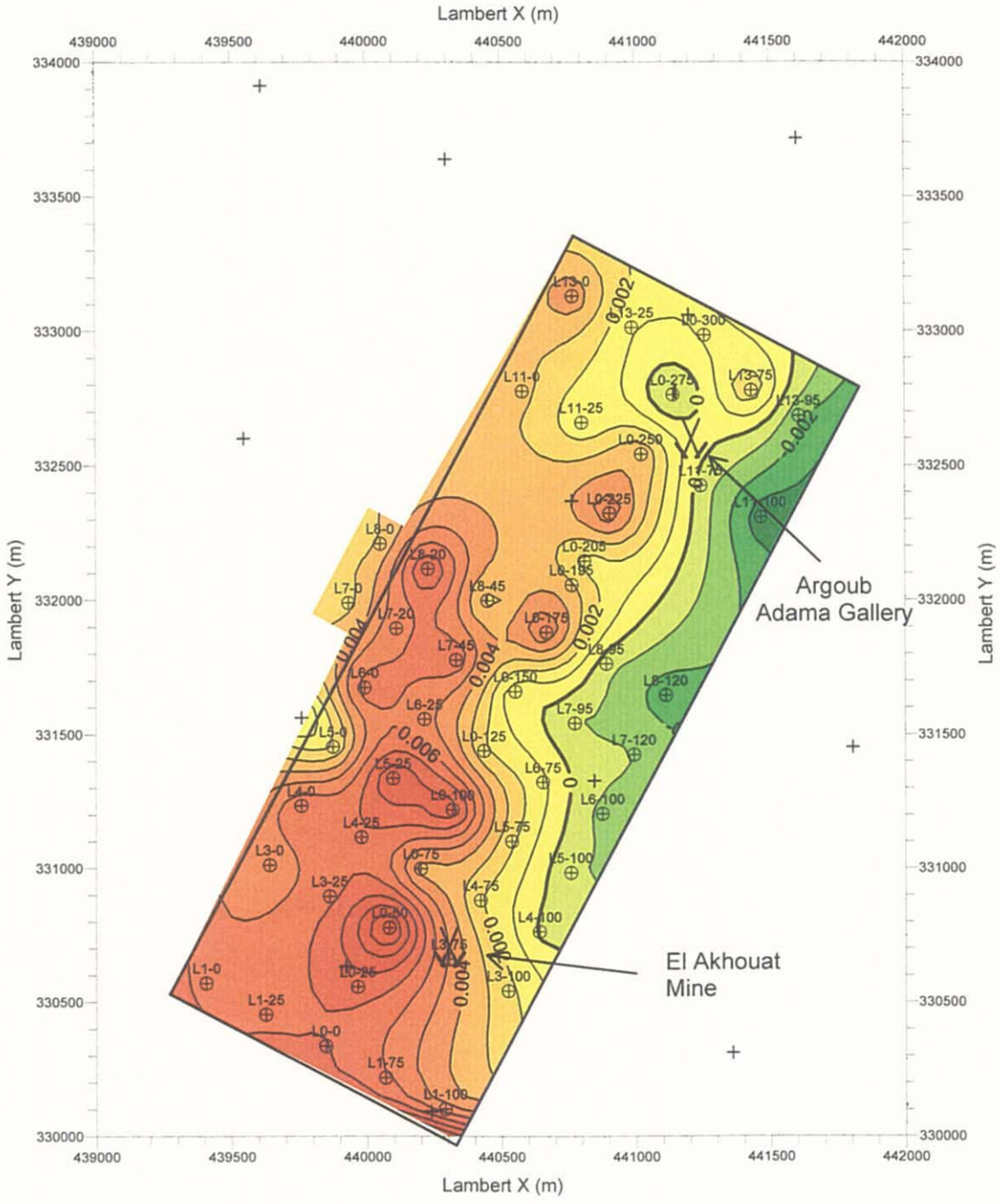

Vertical Derivative Gravity
(mgal/km)

-0.01 -0.008 0.006 0.004 0.002 0 0.002 0.004 0.006 0.008 0.01

Legend

⊕ : Gravity Station

\+ : Existed Gravity Station

□ : Survey Area

XX : Closed Mine

Figure 88

Vertical Derivative Gravity Map in El Akhouat - Argoub Adama area

Scale 1 : 25,000

March, 2000

the site. The old tunnel site of the Argoub-Adama is situated in the zone between high and low anomalies, where the weak fractures are possible to lie with the NW-SE direction.

(5) Cross Sectional Analysis

① Cross Section L0 (Figure 89)

The cross section runs longitudinally the survey site from the SSW to the NNE directions. This section generally consists of two layered model. The high density layer, which is correlated with the Triassic, with density difference of 0.1 to 0.23 g/cm^3 is distributed above the gravity basement with density difference of 0 g/cm^3, which are correlated with the distribution of the Cretaceous limestone.

The lower boundary of surface layer with high density is in depth ranging from 0 to 200m above sea level and its layer thickness is about 200 to 300m. High density layer divides into five blocks, that is, around L0-30 to -70, L0-80 to -150, L0-160 to -200, L0-210 to -250 and L0-270 to -300. The Triassic is not always distributed in the zones between the blocks, where is possible to reflect relative low density due to high porosity caused by the fractures.

The old mine site of the El Akhouat is situated in thick parts of the surface layer with density difference of 0.15 g/cm^3. The old tunnel site of the Argoub-Adama is situated in the surface boundary between the gravity basement and surface layer with high density.

② Cross Section L3 (Figure 90)

The cross section runs through the old mine site of the El Akhouat from the NW to the SE directions. The two layered model in which high density layer with density difference of 0.0-5 to 0.2 g/cm^3 is distributed above the gravity basement with density difference of 0 g/cm^3, is analyzed over whole cross section.

After rising up once to near surface in the vicinity of the old mine site of the El Akhouat, the upper boundary of the gravity basement, which depth is ranging between 0 and 100m above sea level, is exposed at the surface. The gravity basement is correlated with the Triassic in principle and the outcropping gravity basement is correlated with the Tertiary composed of sedimentary rocks in the northwest end of the measuring line. The density difference of surface layer with high density, which is correlated with the Cretaceous limestone, becomes greater in and around the stations L3-40 to -90 on the central hill comparing with northwestern side of the measuring line.

The old mine site of the El Akhouat is situated at the boundary, between the gravity basement and surface high density layer, in the northwestern side of the rising

structure of the gravity basement.

③ Cross Section L4 (Figure 91)

The cross section runs through north-northeast side parallel to the line L3 with 250m spacing. The density section indicates two layered model similar to the previous section L3 and the gravity basement, correlated with the Triassic, rises up to the surface. The outcropping gravity basement in the northwest end of the measuring line is correlated with the Tertiary composed of the sedimentary rocks. The surface layer with high density becomes greater in density and thinner in thickness compared with previous section L3. Its density difference is ranging between 0.15 and 0.27 g/cm^3 and the thickness is ranging between 200 and 300m.

④ Cross Section L5 (Figure 92)

The cross section runs through north-northeast side parallel to the line L4 with 250m spacing. The density section indicates two layered model similar to the previous two sections L3 and L4, however the upper boundary of the gravity basement indicates the different shape. The depth of the gravity basement, which indicates 50m below surface around the northwestern end of the section, becomes deeper up to 200m below surface in and around the station L5-60 and shallower again up to 50m below surface in the southeastern side from near the station L5-70. This rising structure of the gravity basement is considered to reflect the rising structures of the Triassic and/or the distribution of the Tertiary sediment rocks.

The density difference of surface layer, which is correlated with the Cretaceous limestone, is 0.15 g/cm^3 and the thickness of the layer is thin on the hill and thick at the base of hill.

⑤ Cross Section L6(Figure 93)

The cross section runs through north-northeast side parallel to the line L5 with 250m spacing. The density section indicates two layered model similar to the previous section L5. The upper boundary of the gravity basement between the central parts and northwestern end, which depth is ranging from 0 to 200m, becomes shallower up to 200 to 300m above sea level in the southeastern side.

⑥ Cross Section L7 (Figure 94)

The cross section, which is situated at the central parts of the survey area, runs through north-northeast side parallel to the line L6 with 250m spacing. The density section indicates two layered model similar to the previous section L5. The upper boundary of the gravity basement, which depth is greater between the central parts and northwestern end, become shallower up to 100m above sea level in the southeastern side. The gravity basement rising up to near surface in around the station L7-40 becomes deeper up to 100m above sea level around the station L7-30 and

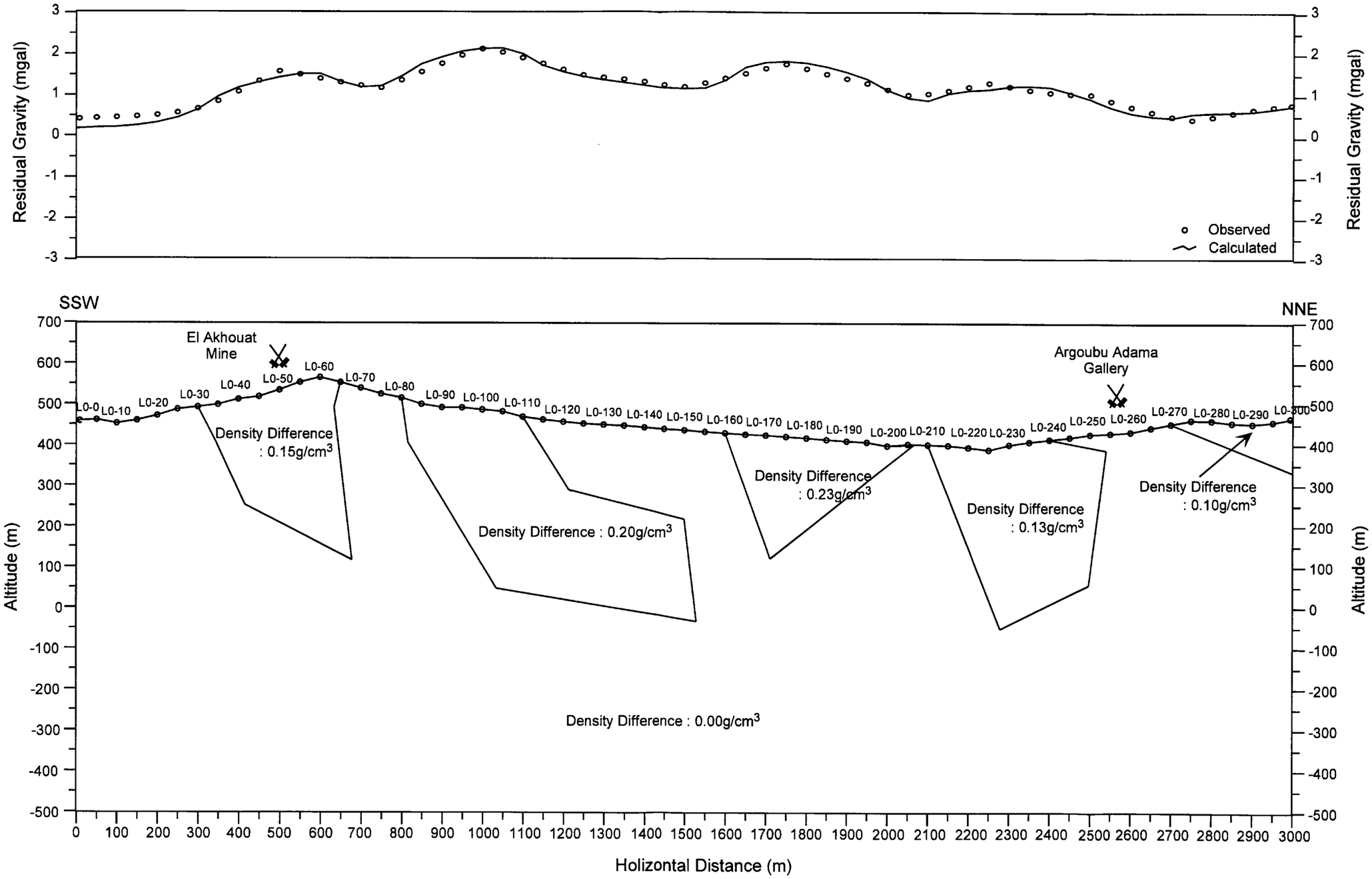

Figure 89
Result of 2-D Gravimetric analysis (Line L0)
Scale : 10,000
March, 2000

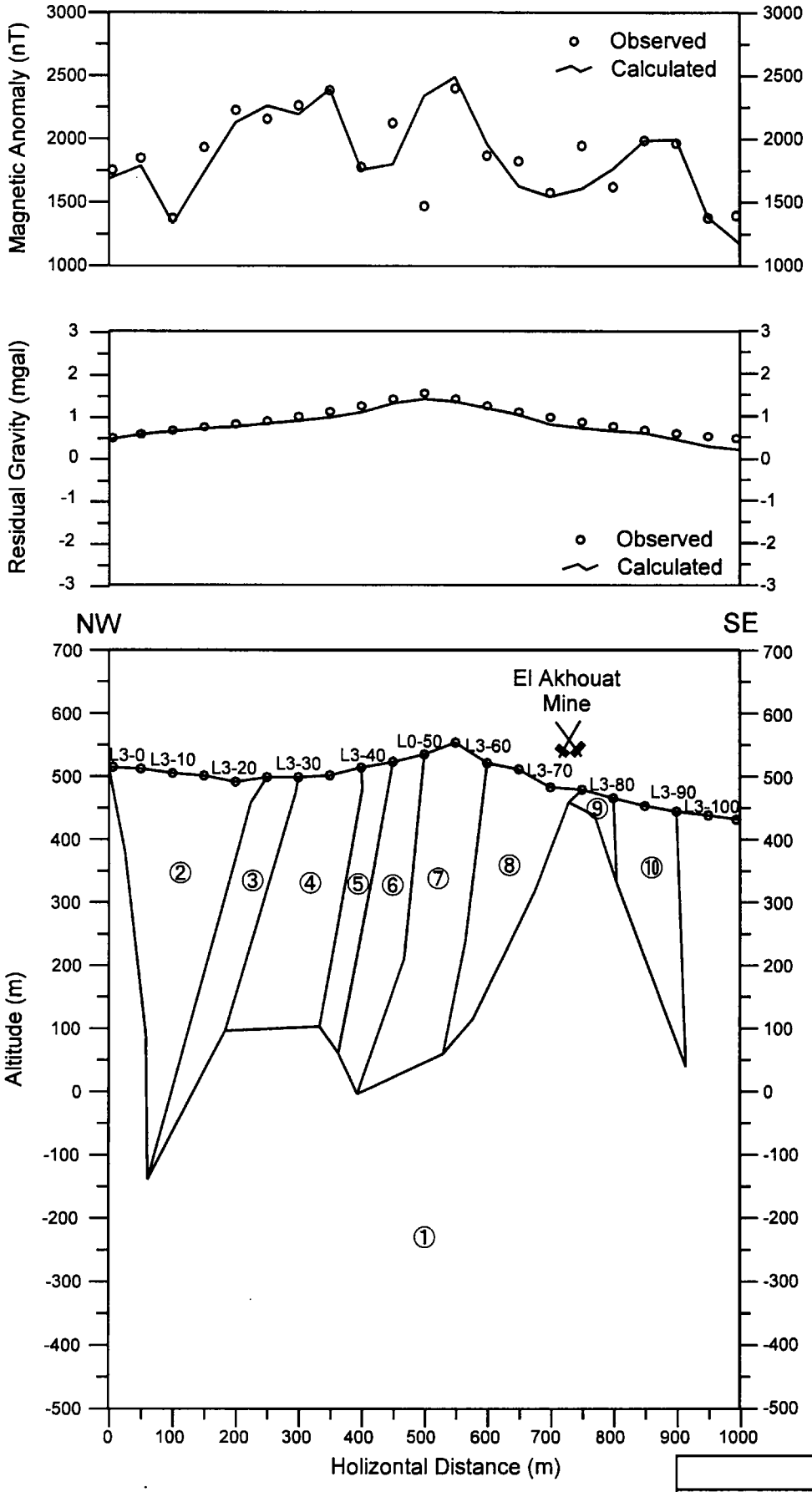

	Density Difference (g/cm³)	Magnetic Susceptibility (cgsemu)
①	0.00	0.000
②	0.05	0.015
③	0.05	0.000
④	0.05	0.025
⑤	0.05	0.000
⑥	0.20	0.015
⑦	0.15	0.000
⑧	0.10	0.070
⑨	0.09	0.000
⑩	0.10	0.050

Figure 90

Result of 2-D Gravimetric and Magnetic analysis (Line L3)

Scale : 10,000

March, 2000

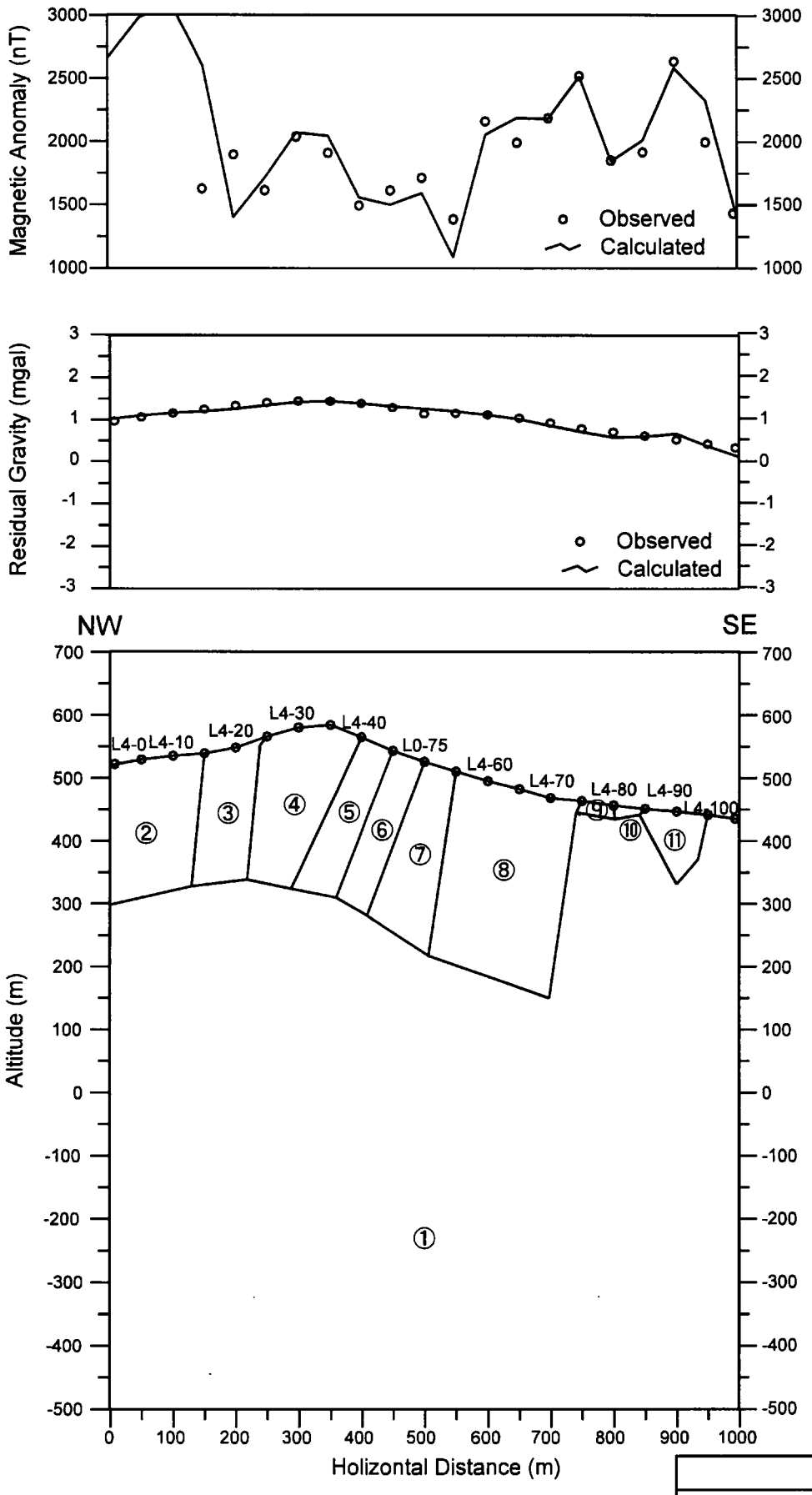

	Density Difference (g/cm³)	Magnetic Susceptibility (cgsemu)
①	0.00	0.000
②	0.15	0.005
③	0.15	0.000
④	0.15	0.002
⑤	0.15	0.000
⑥	0.15	0.003
⑦	0.15	0.000
⑧	0.15	0.004
⑨	0.24	0.005
⑩	0.27	0.000
⑪	0.27	0.005

Figure 91

Result of 2-D Gravimetric and Magnetic analysis (Line L4)

Scale : 10,000

March, 2000

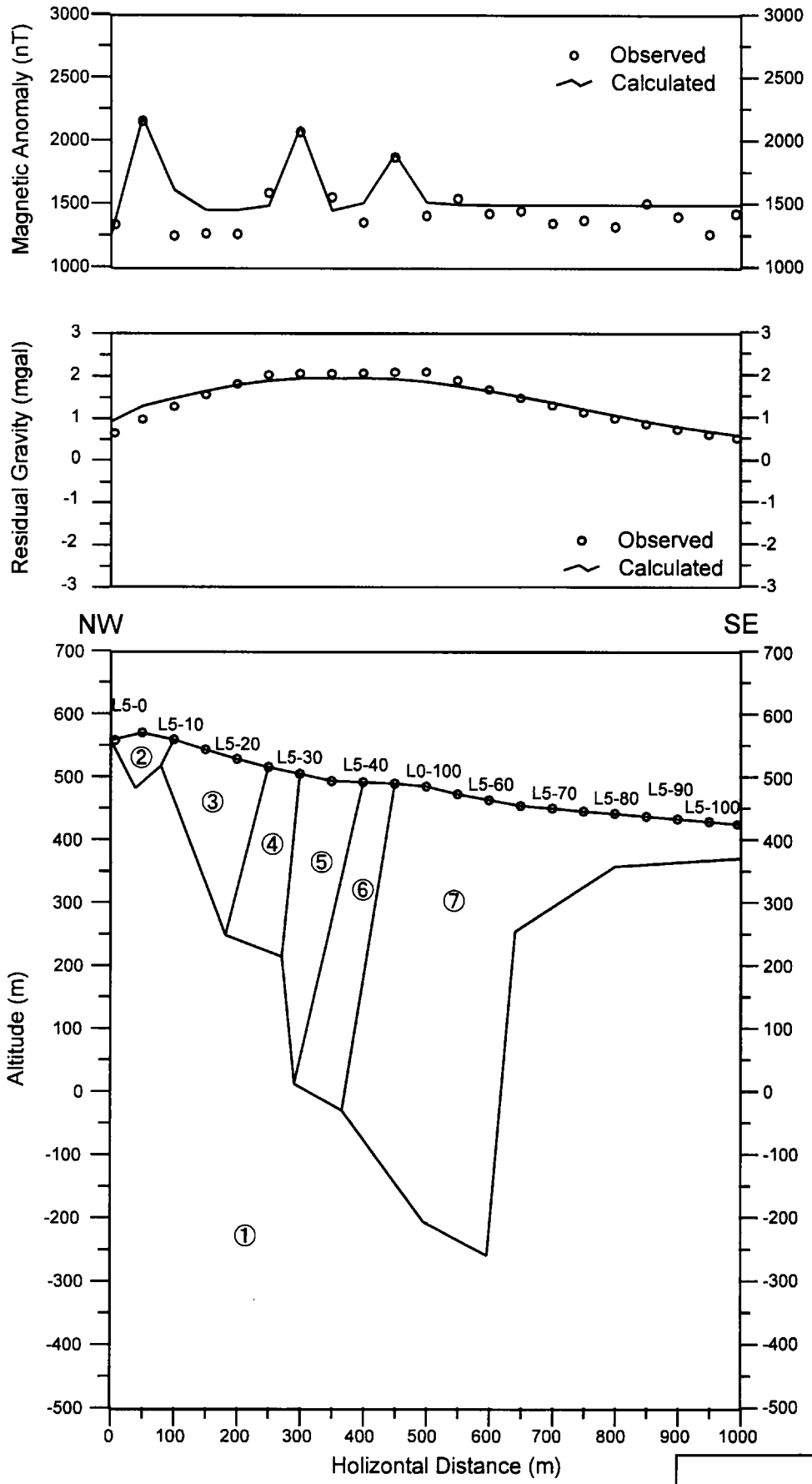

	Density Difference (g/cm³)	Magnetic Susceptibility (cgsemu)
①	0.00	0.000
②	0.15	0.001
③	0.15	0.000
④	0.15	0.001
⑤	0.15	0.000
⑥	0.15	0.002
⑦	0.15	0.000

Figure 92

Result of 2-D Gravimetric and Magnetic analysis (Line L5)

Scale : 10,000

March, 2000

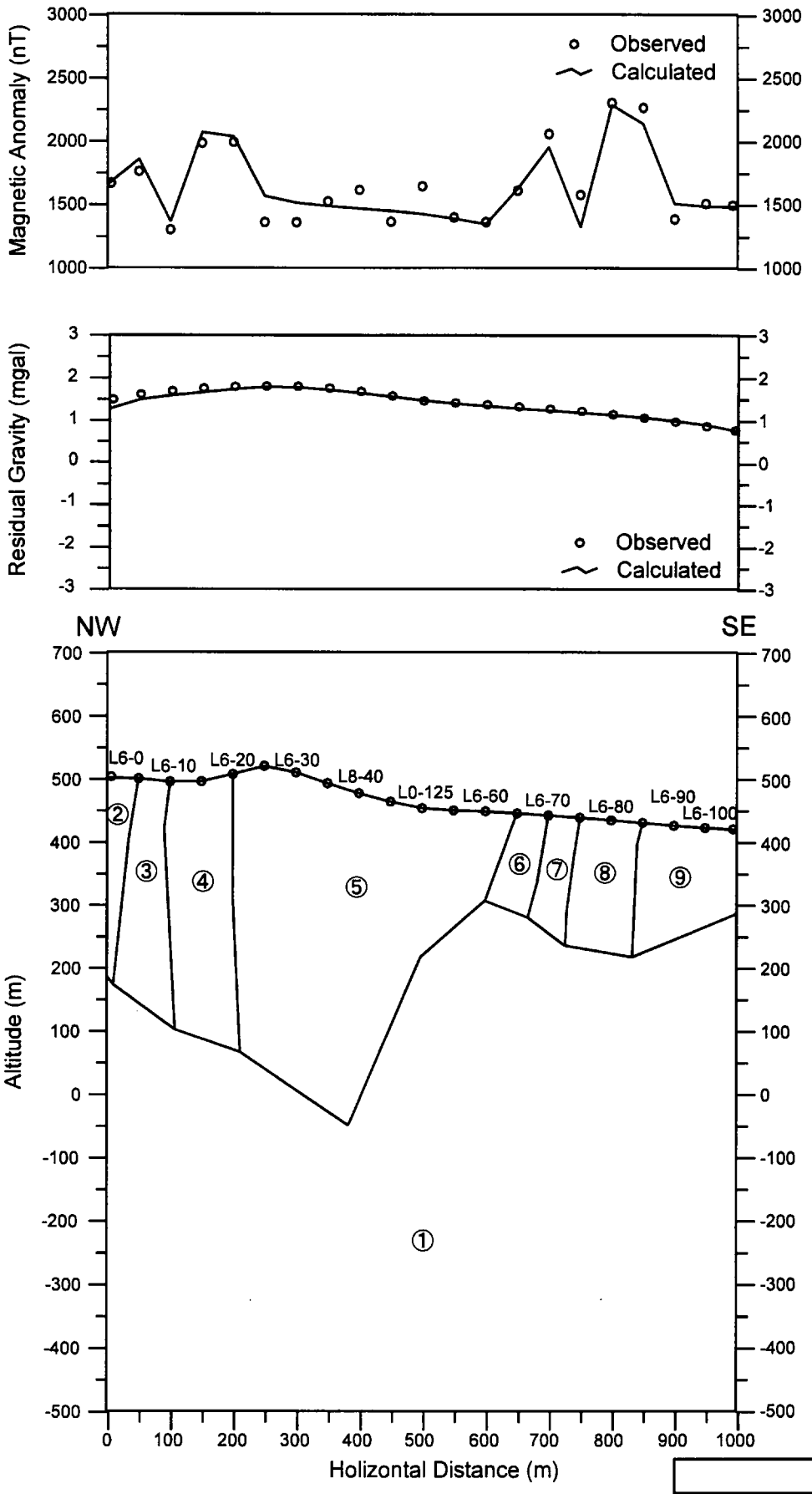

	Density Difference (g/cm^3)	Magnetic Susceptibility (cgsemu)
①	0.00	0.000
②	0.15	0.002
③	0.15	0.000
④	0.15	0.002
⑤	0.15	0.000
⑥	0.15	0.003
⑦	0.15	0.000
⑧	0.15	0.003
⑨	0.15	0.000

Figure 93

Result of 2-D Gravimetric and Magnetic analysis (Line L6)

Scale : 10,000

March, 2000

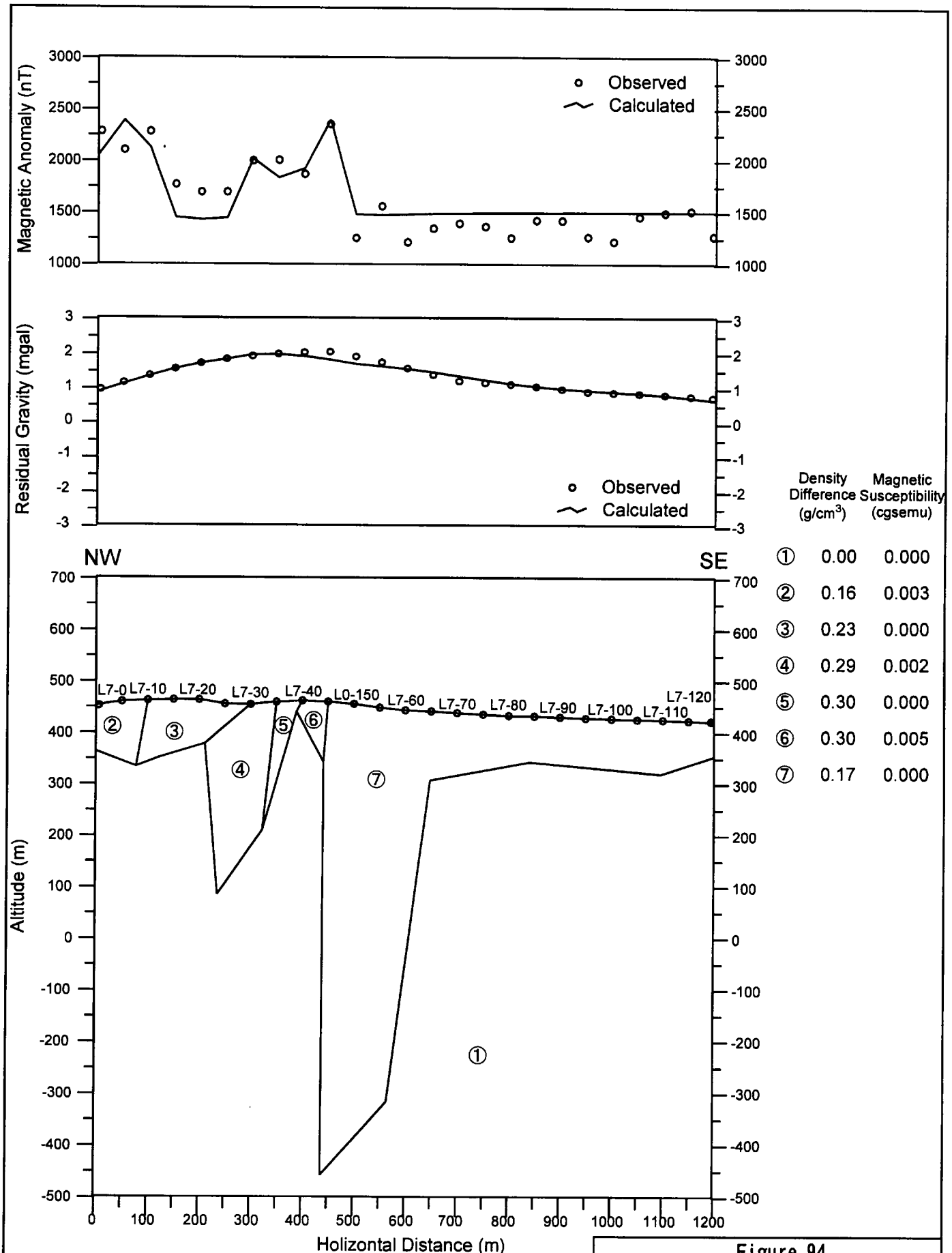

	Density Difference (g/cm^3)	Magnetic Susceptibility (cgsemu)
①	0.00	0.000
②	0.16	0.003
③	0.23	0.000
④	0.29	0.002
⑤	0.30	0.000
⑥	0.30	0.005
⑦	0.17	0.000

Figure 94

Result of 2-D Gravimetric and Magnetic analysis (Line L7)

Scale : 10,000

March, 2000

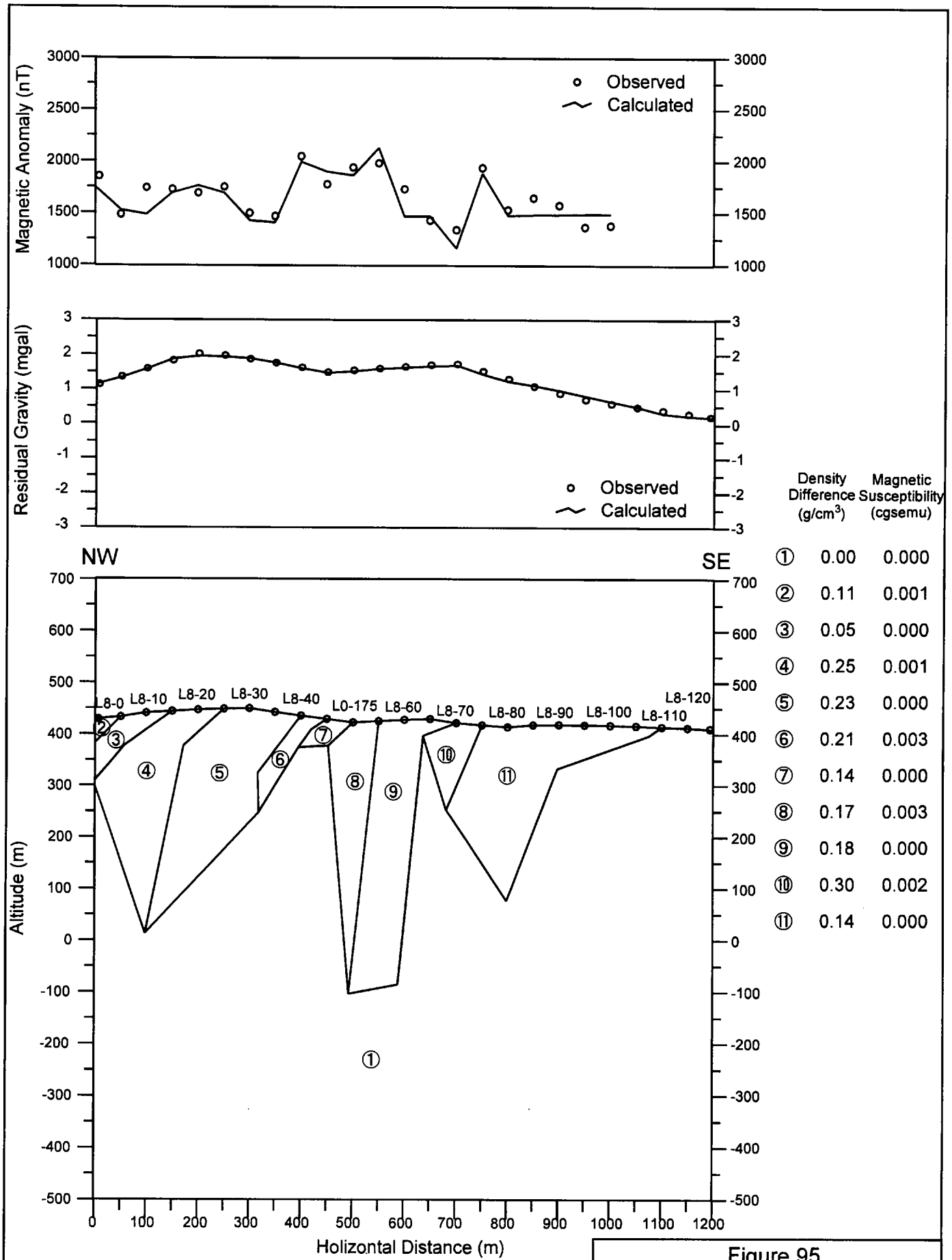

	Density Difference (g/cm^3)	Magnetic Susceptibility (cgsemu)
①	0.00	0.000
②	0.11	0.001
③	0.05	0.000
④	0.25	0.001
⑤	0.23	0.000
⑥	0.21	0.003
⑦	0.14	0.000
⑧	0.17	0.003
⑨	0.18	0.000
⑩	0.30	0.002
⑪	0.14	0.000

Figure 95

Result of 2-D Gravimetric and Magnetic analysis (Line L8)

Scale : 10,000

March, 2000

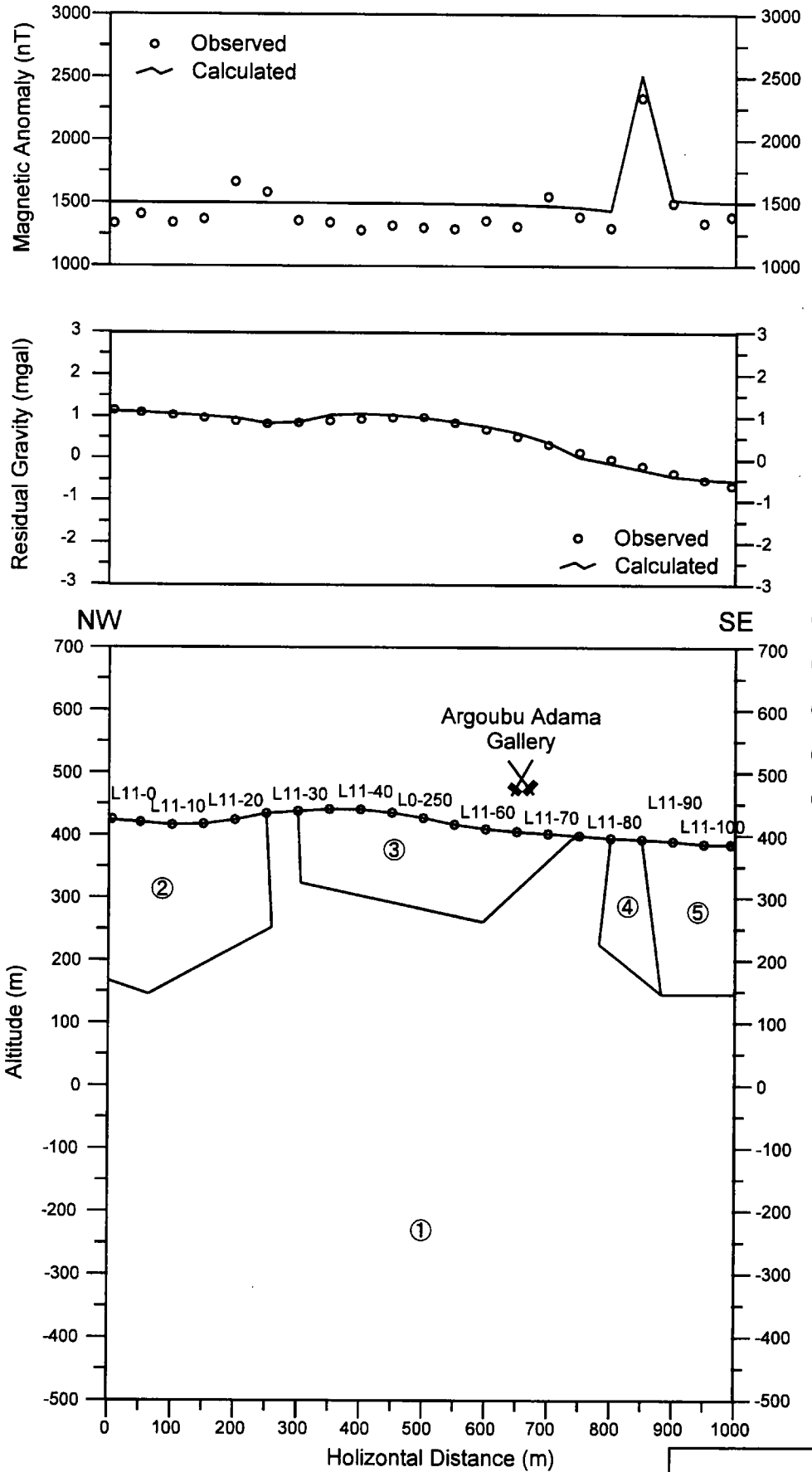

	Density Difference (g/cm^3)	Magnetic Susceptibility (cgsemu)
①	0.00	0.000
②	0.15	0.000
③	0.21	0.000
④	0.00	0.001
⑤	-0.08	0.000

Figure 96

Result of 2-D Gravimetric and Magnetic analysis (Line L11)

Scale : 10,000

March, 2000

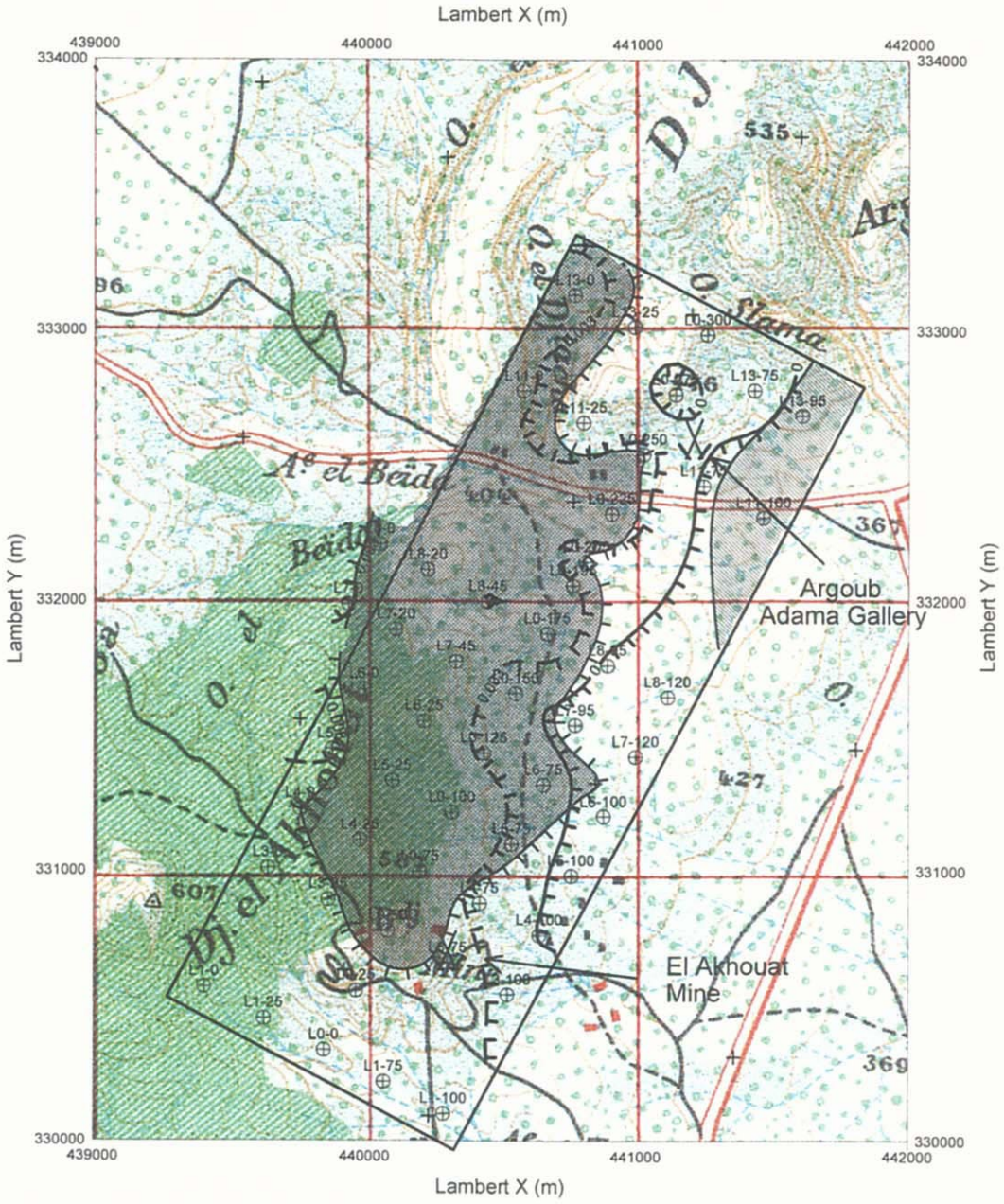

Legend

⊕ : Gravity Station

\+ : Existed Gravity Station

□ : Survey Area

XX : Closed Mine

High Residual Gravity > 1 mgal

Low Residual Gravity < 0 mgal

TTT Vertical Derivative Gravity : 0 mgal/km

T T 1 Vertical Derivative Gravity : 0.003 mgal/km

Figure 97

Gravity Interpretation Map in El Akhouat - Argoub Adama area

Scale 1 : 25,000

March, 2000

shallower again to 100m below surface in the northwestern end. The rising structure around the station L7-40 is correlated with the distribution of the Triassic. The surface layer correlated with the Cretaceous limestone indicates the density difference ranging from 0.16 to 0.17 g/cm^{3}and becomes greater up to the density difference ranging from 0.23 to 0.3 g/cm^3 in the vicinity of the rising structure of gravity basement between the station L7-10 and L7-50.

⑦ Cross Section L8 (Figure 95)

The cross section, which is situated at the central parts of the survey area, runs through north-northeast side parallel to the line L7 with 250m spacing. The upper boundary of gravity basement, which is correlated with the Triassic, rises up to near surface around the stations L8-40 and L8-70 and becomes shallower in the southeastern side from the station L8-10 and exposes on the surface in the southeastern end of the section. The gravity basement in the southeastern parts is correlated with the sedimentary rocks of the Tertiary.

The density difference of surface layer with high density varies strongly ranging from 0.05 to 0.3 g/cm^3 and its thickness is about 400m except the gravity rising zone.

⑧ Cross Section L11 (Figure 96)

The cross section runs through northern parts of the survey site from the NW to the SE directions. Two layered model in which the high density layer with density difference of 0.15 to 0.21 g/cm^3 is distributed above the gravity basement. Lower density layer correlated with the Tertiary sediment rocks is distributed on the surface. The distribution extent of high density layer is associated with distribution extent of the Triassic and the density variations within the layer are considered to reflex the difference of the rocks within the Triassic.

(6) Plane Analysis

The first vertical derivative plan with contours of 0 mgal/km and 0.003 mgal/km over the characteristic distribution plan of gravity residual is shown in Figure 97.

The old mine sites of the El Akhouat and the Argoub-Adama are located in and around the narrow zone of steep gravity gradient, where the high gravity residual exceeding 1mgal decreases rapidly to low gravity residual in the eastern parts of the survey area. It is considered that the anomaly of this high gravity residual is caused by the Cretaceous limestone layer with high density and the low density layer in the eastern side are caused by the Tertiary sediments. A constricted part of the local gravity residual low is observed in the eastern parts within high gravity residual and